Characterising antibody kinetics from multiple influenza infection and vaccination events in ferrets

James A. Hay[1], Karen Laurie[2,3], Michael White[4], Steven Riley[1*]

1 MRC Centre for Global Infectious Disease Analysis, Department of Infectious Disease Epidemiology, Imperial College, London, UK

2 WHO Collaborating Centre for Reference and Research on Influenza, Peter Doherty Institute for Infection and Immunity, Melbourne, Australia

3 Seqirus, 63 Poplar Road, Parkville Victoria 3052, Australia

4 Malaria: Parasites and Hosts, Department of Parasites and Insect Vectors, Institut Pasteur, Paris, France

* s.riley@imperial.ac.uk

Abstract

The strength and breadth of an individual's antibody repertoire are important predictors of their response to influenza infection or vaccination. Although progress has been made in understanding qualitatively how repeated exposures shape the antibody mediated immune response, quantitative understanding remains limited. We developed a set of mathematical models describing short-term antibody kinetics following influenza infection or vaccination and fit them to haemagglutination inhibition (HI) titres from 5 groups of ferrets which were exposed to different combinations of trivalent inactivated influenza vaccine (TIV with or without adjuvant), priming inoculation with A/H3N2 and post-vaccination inoculation with A/H1N1. Based on the parameter estimates of the best supported model, we describe a number of key immunological features. We found quantifiable differences in the degree of homologous and cross-reactive antibody boosting elicited by different exposure types. Infection and adjuvanted vaccination generally resulted in strong, broadly reactive responses whereas

unadjuvanted vaccination resulted in a weak, narrow response. We found that the order of exposure mattered: priming with A/H3N2 improved subsequent vaccine response, and the second dose of adjuvanted vaccination resulted in substantially greater antibody boosting than the first. Although there was considerable uncertainty in our estimates of antibody waning parameters, our results suggest that both short and long term waning were present and would be identifiable with a larger set of experiments. These results highlight the potential use of repeat exposure animal models in revealing short-term, strain-specific immune dynamics of influenza.

Author summary

Despite most individuals having some preexisting immunity from past influenza infections and vaccinations, a significant proportion of the human population is infected with influenza each year. Predicting how an individual's antibody profile will change following exposure is therefore useful for evaluating which populations are at greatest risk and how effective vaccination strategies might be. However, interpretation of antibody data from humans is complicated by immunological interactions between all previous, unobserved exposures in an individual's life. We developed a mathematical model to describe short-term antibody kinetics that are important in building an individual's immune profile but are difficult to observe in human populations. We validated this model using antibody data from ferrets with known, varied infection and vaccination histories. We were able to quantify the independent contributions of various exposures and immunological mechanisms in generating observed antibody titres. These results suggest that data from experimental systems may be included in models of human antibody dynamics, which may improve predictions of vaccination strategy effectiveness and how population susceptibility changes over time.

Introduction

Natural infection with influenza stimulates a multifaceted immune response to control virus replication and ultimately clear the infection. [1] The adaptive immune response is of particular interest for seasonal epidemic and pandemic preparedness, as it provides

some long-term protection against reinfection and disease via antibody and T-cell mediated immunity. [2–5] However, influenza undergoes continual antigenic drift, during which mutations in immunodominant epitopes are selected for under immunological pressure, allowing influenza lineages to escape herd immunity. [6–8] This results in the waning of long-term immunity as antibodies effective against past strains fail to neutralize novel variants. [9] Consequently, the seasonal influenza vaccine is regularly updated to better represent circulating strains. [10, 11] Whilst there is some limited cross-reactivity and cross-protection within influenza A virus subtypes and within influenza B virus lineages, incomplete protection means that humans experience numerous infections over their lives. [12–14].

Each successive influenza exposure, which may be vaccination or infection, can strengthen the available repertoire of T and B cells which target circulating and previously encountered strains. [15, 16] In the humoral response, this occurs by temporarily boosting levels of preexisting antibodies and by inducing a B cell response against the new strain. [17–19] In the case of influenza, where individuals experience repeated infections and vaccinations from antigenically varied viruses, interpretation of an observed antibody response is confounded by the complex interaction of an individual's preexisting immunity with the infecting virus. [20, 21] A large body of experimental and observational work exists describing the contribution of these interactions to observed influenza susceptibility profiles and antibody landscapes. [1, 22–26] However, few studies have integrated these mechanisms into quantitative frameworks which can be used to explain and predict serological data from human populations. [14, 18, 27, 28]

Animal models, in particular ferrets, have been used to generate much of our understanding of influenza immunology due to opportunity for intensive observation and control. [29–35] Here, we exploit the experimental flexibility and transparency of a ferret model to find evidence for and quantify multiple immunological mechanisms that may be important in characterizing antibody landscapes generated from complex exposure histories. Quantifying short term mechanisms in a ferret system might reveal patterns that could be used to improve the predictability and interpretation of human antibody landscapes following exposure. [36]

We developed a mathematical model of antibody boosting and biphasic waning to

describe antibody kinetics in a group of ferrets with varied but known exposure histories. The model takes into account previously described immunological phenomena to describe antibody titres arising from any exposure history. By fitting this model to haemagglutination inhibition (HI) titre data in these ferrets, we sought to quantify the impact of prior infection and adjuvant inclusion on antibody levels following vaccination, as well as to compare homologous and cross reactive boosting profiles of different exposure types. [37–41] We considered previously described short-term dynamics that are conditional on both (i) time since exposure and (ii) exposure types that are yet to be included in models of antibody landscapes. [14, 17]

Materials & Methods

Study Data

Fifteen ferrets were each assigned to one of five experimental groups, with each group comprised of three ferrets. [29] These ferrets underwent different combinations of infection with seasonal influenza A and/or vaccination with Northern and Southern Hemisphere trivalent inactivated influenza vaccine (TIV), with or without Freund's incomplete adjuvant, over the course of 70 days (Table 1). Serum samples were collected at days 0, 21, 37, 49 and 70 from all ferrets (Fig 1). HI titres were used to determine antibody titres to each infection and TIV strain. Dilution plates with 12 wells were used, such that the highest possible recorded dilution was 1:40960, and the lowest detectable titre was 1:20. Undetectable titres were recorded as <1:20. Data were then transformed to a $\log_2$ scale such that observable titres were assigned values between 0 and 12, where <1:20 was treated as 0.

Full adult doses of human TIV were used in groups A, B, C and D. The first TIV was the Southern Hemisphere 2008 TIV, containing A/Solomon Islands/3/2006 (H1N1), A/Brisbane/10/2007 (H3N2) and B/Brisbane/3/2007 at day 28 (TIV 1). The second vaccination was the Northern Hemisphere 2007/2008 TIV, containing A/Solomon Islands/3/2006 (H1N1), A/Wisconsin/67/2005 (H3N2) and B/Malaysia/2506/2004 at day 42 (TIV 2). Vaccines used in groups B and D were also emulsified in an equal volume of Freund's incomplete adjuvant immediately before administration (TIV 1/2 +

adjuvant). All vaccines contained 15μg of HA from each strain, and were delivered to sedated animals intramuscularly in the quadriceps muscles of both hind legs. Infections were carried out by dropwise intranasal challenges with infectious doses of A/Panama/2007/1999 (H3N2) in groups C, D and E, and with A/Fukushima/141/2006 (H1N1) in all groups.

Table 1. Description of experimental protocol.

Group	Infection with A/Panama/2007/99 (H3N2)	Immunisation with S.H TIV 2008*	Immunisation with N.H TIV 2007/2009**	Infection with A/Fukushima/141/06 (H1N1)
Group A	No	Yes (no adjuvant)	Yes (no adjuvant)	Yes
Group B	No	Yes (with adjuvant)	Yes (with adjuvant)	Yes
Group C	Yes	Yes (no adjuvant)	Yes (no adjuvant)	Yes
Group D	Yes	Yes (with adjuvant)	Yes (with adjuvant)	No
Group E	Yes	No	No	Yes

*Southern Hemisphere (S.H.) TIV 2008: A/Solomon Islands/3/2006 (H1N1), A/Brisbane/10/2007 (H3N2), B/Brisbane/3/2007

**Northern Hemisphere (N.H.) TIV 2007/2008: A/Solomon Islands/3/2006 (H1N1), A/Wisconsin/67/2005 (H3N2), B/Malaysia/2506/2004

The experimental protocol was designed originally to reflect different possible human infection and vaccination histories at the time of the 2009 pandemic. [29] Here we present a secondary analysis of these data, with the intention of characterizing underlying immunological processes.

Models of antibody kinetics

The model describes the kinetics of homologous and heterologous antibody titres following exposure. Fig 2 depicts the example of an individual becoming infected and later vaccinated, though the model may characterise any sequence of exposures. After infection (star at time ξ_1), homologous antibody titres undergo boosting rising linearly to a peak after time t_{p1}. Titres then quickly drop by a fixed proportion, d_1, as the short-lived component of the antibody response wanes over time t_{s1}. Antibody titres then enter a long-term, slower waning phase at rate m_1 until subsequent vaccination (syringe at time ξ_2), when antibody dynamics become dominated by a new set of boosting and waning parameters. Antibodies effective against heterologous strains experience boosting and biphasic waning in parallel, though to a smaller degree depending on the antigenic similarities of the measured and exposure strains.

Various iterations of the model were developed to incorporate different immunological mechanisms that might be important in describing antibody boosting and waning. Each combination of model assumptions was fit to the data, and a model comparison analysis was undertaken to identify those mechanisms that were best supported. These included: biphasic or monophasic antibody waning; exposure-type specific or type non-specific cross-reactivity; antigenic seniority; the impact of priming infection on subsequent vaccine response; and titre-dependent boosting. We also considered models with either 3 (infection, TIV, TIV + adjuvant) or 6 (priming infection, secondary infection, initial TIV, secondary TIV, initial TIV + adjuvant, secondary TIV + adjuvant) distinct exposure types. Results shown in Fig 3- 5 are from the model variant that was best supported by the model comparison analysis based on the Watanabe-Akaike Information Criterion (WAIC). Full details of the methods and all model variants used are described in Supporting Protocol S1. All code and data are available as an R package at https://github.com/jameshay218/antibodyKinetics.

Results

Variation in antibody kinetics driven by different exposures

The raw data show substantial variation in observed antibody titres across the groups driven by different exposure types and combinations. Following two doses of unadjuvanted TIV, ferrets achieved only modest increases in titres against the vaccine strains (Fig 3A), with 2 out of 3 ferrets failing to generate H3N2 titres that persisted past day 37. The addition of an adjuvant resulted in increased and persistent titres against the vaccine strains and A/Fukushima/141/2006 (H1N1) in all ferrets by day 49, despite no ferret having been exposed to A/Fukushima/141/2006 (H1N1) at that time (Fig 3B). Similarly, priming infection resulted in higher and long-lived titres to the vaccine strains and A/Fukushima/141/2006 (H1N1) relative to ferrets in the unprimed, unadjuvanted TIV protocol (Fig 3C). Observed titres at day 21 against A/Panama/2007/1999 (H3N2) were consistently high following priming infection in groups C-E, with one ferret in each of groups C and E also experiencing some boosting of antibodies against the other H3N2 strains. All ferrets were infected with

A/Fukushima/141/2006 (H1N1) at day 56, leading to elevated titres to both H1N1 strains by day 70 in all ferrets. Overall, ferrets that received more frequent and immunogenic exposures achieved the highest, most broadly reactive and long-lived antibody titres.

The parameters of the best fitting model suggest: a role for priming infection in increasing subsequent vaccine response; different boosting profiles between vaccination and infection; different boosting profiles with adjuvant versus without adjuvant; biphasic antibody waning; exposure-type specific cross-reactivity parameters; and decreasing antibody boosting with each successive exposure (antigenic seniority). We did not find evidence for titre-dependence in modifying antibody boosting from higher or lower preexisting titres (Fig S3). Fig 3 shows the best performing model fit to the data (the remainder of the results refer to estimates from this model, with parameter estimates given in Table S3). Model variants were compared based on both their goodness-of-fit and parsimony (WAIC value), and the combination of mechanisms included in this best-fitting model are therefore considered to be well supported by the data. The sensitivity of parameter estimates to different model assumptions are discussed in Supporting Protocol S1.

Comparison of homologous boosting by exposure type

The level of homologous boosting resulting from priming infection (Infection 1) and secondary infection (Infection 2) appeared to be similar after accounting for exposure order (Infection 2 was the second, third and fourth exposure in groups E, A/B and C/D respectively). Similar estimates were obtained for μ from both infections (Fig 4A). The antibody response following priming infection appeared to be persistent. We inferred that antibody titres fell only marginally following the initial waning phase ($\mu(1-d)$, Fig 4B). The antibody waning rate was not identifiable for secondary infection due to the lack of observations following this exposure. We found evidence for only low levels of homologous antibody boosting following both initial and secondary doses of unadjuvanted TIV (TIV 1 and TIV 2) that quickly waned to near undetectable levels during the initial waning phase.

The addition of an adjuvant appeared to have no significant impact on the

homologous antibody response to the first vaccine dose, but did improve the response to a second dose of vaccine (TIV 1 compared to TIV 1 + adjuvant and TIV 2 compared TIV 2 + adjuvant, Fig 4B). Titres against A/Brisbane/10/2007 (H3N2) and A/Solomon Islands/3/2006 (H1N1) were similar following the first unadjuvanted vaccine dose and the first adjuvanted vaccine dose (TIV 1 compared to TIV 1 + adjuvant, Fig 3A&B). However, the second adjuvanted TIV dose appeared to elicit a significant persistent boost to the vaccine strains, which resulted in peak titres near the limit of detection of this assay (TIV 2 compared to TIV 2 + adjuvant, Fig 3A&B).

Comparison of cross reactivity by exposure type

We found differences in the amplitude of cross reactivity elicited by the 6 exposure types shown in Fig 4. Secondary infection appeared to elicit a level of cross reactivity in line with that of the priming infection, whereas cross reactivity for both unadjuvanted and adjuvanted vaccination appeared to be narrower (Fig 5). These results suggest that secondary infection elicited broadly reactive antibody boosting similar to priming infection, whereas the antibody response following vaccination only boosted antibodies that were effective against antigenically similar viruses. The cross reactivity gradient parameter, σ, could not be identified for the second dose of unadjuvanted TIV and first dose of adjuvanted TIV, and we were only able to recover the prior distribution for these parameters. These values were therefore excluded from Fig 4B. Fig 5 demonstrates that the reason for this lack of identifiability may be that homologous boosting (the y-intercept) was too small to elicit any measurable cross reactive boosting at these antigenic distances. When a single cross reactivity gradient was assumed for all exposure types, we estimated the cross reactivity gradient to be 2.44 (mean; 95% CI: 1.64 - 3.28), suggesting a narrower cross reactivity than would be expected given the definition for cross reactivity based on ferret antisera (an antigenic distance of 1 unit should see a reduction in antibody boosting of 1 log titre unit).

Magnitude and duration of waning phases

Our model provided support for the presence of an initial short-term, rapid waning phase followed by a secondary long-term, sustained waning phase. For all vaccine doses,

we estimated that the majority of the antibody boost waned within 10 days of reaching the peak (upper 95% credible interval (CI) <10 days for all TIV estimates, Fig 4C&D). Conversely for priming infection, we estimated that the antibody titre was maintained at near peak levels with an estimated initial waning phase duration of 16.1 days (mean; 95% CI 6.24 - 19.8) and a 15.9% (mean; 95% CI: 1.30 - 35.4%) drop in log titre relative to the peak. We estimated similar long-term waning rates for second unadjuvanted TIV, second adjuvanted TIV and priming infection (Fig 4).

Impact of priming

Prior to receiving non-adjuvanted TIV, experimental group C was infected with H3N2 Panama/2007/1999 at day 0, which represented a host being primed by natural infection prior to vaccination. Our model allowed us to identify additional homologous and cross-reactive antibody boosting that resulted from priming improving the subsequent vaccine response, as comparable experimental groups were given the same vaccination schedule with or without priming infection. We found that priming infection resulted in a significant additional boost to antibodies against the A/H1N1 and A/H3N2 vaccine strains at the time of vaccination in addition to that provided by the vaccine itself (Fig 4A).

We estimated the cross reactivity of this additional boost to be broad with a gradient of 0.690 (mean; 95% CI: 0.400 - 1.12), suggesting that priming increases the cross-reactive breadth of the vaccine response. It should be noted that whilst additional priming-induced vaccine boosting is well supported by the model fit, the model overestimates the antibody titre to A/Fukushima/141/2006 (H1N1) at day 37 elicited by initial dose of TIV following priming by H3N2 infection (Fig 3C). This may be a result of subtype-specific interactions that are not captured by our model.

Limited evidence for antigenic seniority

We found some evidence for a trend of decreasing antibody response with increasing number of prior exposures. We found a general trend for a decrease in the scaling parameters ρ_2, ρ_3, and ρ_4 with each subsequent exposure. Assuming that the first exposure results in a full boost ($\rho_1 = 1$), we estimated ρ_2 to be 0.824 (mean; 95% CI:

0.686 - 0.971), ρ_3 to be 0.769 (mean; 95% CI: 0.583 - 0.960), and ρ_4 to be 0.279 (mean; 95% CI: 0.0710 - 0.499) for the second, third and fourth exposures respectively.

Discussion

In this study, we used a mathematical model of antibody kinetics to describe boosting and waning following influenza vaccination or infection in a group of well characterized ferrets. We fit various subsets of the model with different immunological mechanisms to the data and found that the best supported model included: type-specific antibody boosting; antigenic distance-mediated cross reactivity specific to each exposure type; type-specific biphasic waning; 6 distinct exposure types; antigenic seniority; and a role for priming in increasing subsequent vaccine response. We identified quantitative differences in the level of homologous and cross-reactive antibody boosting between vaccination, infection and adjuvanted vaccination in this ferret model. A single TIV dose with or without adjuvant elicited negligible levels of homologous and cross reactive boosting. A second dose of TIV with adjuvant resulted in significant, broadly reactive antibody boosting, whereas a second dose of TIV without adjuvant did not elicit significant antibody boosting. The profile of boosting for primary infection was consistent across experimental groups, and similar in magnitude to secondary infection. Furthermore, we found that priming infection induced a significantly broader and stronger boosting profile following subsequent vaccination.

Although there are limitations in applying results from animal models directly to humans, these mechanisms may also apply in the human immune response and be important in accurately capturing human antibody dynamics at a short time scale. [18] Our results suggest that mathematical models of antibody kinetics that explicitly consider immunological mechanisms and exposure-type specific parameters would be valuable for the prediction of antibody landscapes in human populations. Although direct inference from long-term observational data in humans may be difficult, experimental models, such as the ferret system described here, provide an excellent alternative data source for the inference of short-term immunological mechanisms that may map onto models recovered using human sera. [14, 17, 27, 28]

Our work has a number of limitations. First, we had insufficient power to quantify

all of the mechanisms proposed here. We therefore restricted our conclusions to mechanisms that were supported based on their recurrence across a set of 10 supported model variants (Supporting Protocol S1). Also, the frequency at which blood samples were taken compared to the number of exposure events resulted in a relatively small amount of data given the number of mechanisms being explored. In particular, sampling around the biphasic waning period of the vaccinations and following the final exposure event was limited, resulting in poor identifiability for some of these model parameters. Nonetheless, we found evidence for biphasic waning following secondary vaccination and primary infection based on the constrained parameter estimates for TIV 2, TIV 2 + adjuvant and primary infection.

Experiments of a similar design with fewer exposures and more frequent sampling would power the model to elucidate these waning phases further. Although studies of antibody response duration have been carried out in humans, quantifying waning rates independent of interfering subsequent and past exposures is difficult. [42, 43] Further mechanisms such as differential waning rates between cross-reactive and homologous antibodies or titre-dependent ceiling effects are likely to be important, but were not identifiable here. [17, 44] There may also be underlying heterogeneities in antibody response between and within influenza subtypes. [45] It would be interesting to investigate the use of this model to compare antibody kinetics for different vaccine and adjuvant types. [46] For example, Live Attenuated Influenza Vaccines (LAIV), as well as newer DNA vaccines may provide different antibody kinetic profiles and may elicit broader antibody responses, or provide different priming effects. [47, 48]

Our results have implications for comparing different vaccination strategies. Achieving high HI titres against currently circulating strains is a key endpoint in influenza vaccine trials due to its correlation with clinical protection. [4, 49–51] However, there are a number of obstacles to achieving these high titres in some populations including antigenic interactions, age specific responses and antibody waning. [9, 52–55] A practical approach to improving vaccine effectiveness is therefore to elicit a broader antibody response to compensate for potential strain mismatch. [56] Adding adjuvants such as MF59 and AS03 has been shown to induce higher antibody titres that have greater cross-reactive properties. [40, 41, 57, 58] Quantitative comparisons of cross reactivity profiles, as we have provided here, would be a useful tool in comparing the

effectiveness of different adjuvants, which would provide a measurable benefit to trade-off against safety and immunogenicity concerns. [59, 60]

"Prime-boosting" is another strategy that aims to induce a broadly protective immune response in the context of pandemic preparedness. [37, 38, 61] Our work supports previous observations that natural infection with influenza acts as a form of priming. [39] Although the phylogenetic relationship between the priming and subsequent boosting strain is likely to be important, priming has been shown previously to occur between subtypes in animal models. [31–33] Experimental models using analytical methods such as those presented here would help to quantify the interaction of natural infection and influenza vaccination, as well as the potential priming effects from different influenza vaccine types.

Fig 1. Summary of experimental protocol. Days since first event are shown on the x-axis, with the 5 groups shown as rows. Red stars represent infection with either A/Panama/2007/1999 (H3N2) or A/Fukushima/141/2006 (H1N1). Red circles represent vaccination with either Southern Hemisphere TIV 2008 (TIV 1) or Northern Hemisphere TIV 2007/2008 (TIV 2) with (grey border) or without (black border) adjuvant. Vertical, dashed red lines represent times of blood sample collection, providing HI titres against each of the vaccination and infection strains at that time point.

Fig 2. Base model. Schematic showing the relationship between model parameters and antibody kinetics over time. After each exposure, antibody levels undergo linear boosting on a log scale followed by an initial, short waning phase and then a slower, long-term waning phase. This example demonstrates two exposures, initially with infection (star symbol) and subsequently with vaccine (syringe symbol), where antibody dynamics are governed by a set of parameters depending on the exposure type. Note that the y-axis is on a log scale and all real measurements are observed as discrete and taken as the floor value. The grey line highlights how antibody levels to a different influenza antigen develop in parallel driven by exposure to the heterologous (black line) strain. Model parameters are described in Table S1.

Fig 3. Model trajectory fits. Colored lines represent the best-fit trajectories of antibody kinetics following exposure. Coloured shaded regions show 95% credible intervals of the model fit. Colored points show observed discrete log antibody titres by HI assay for each of the three individual ferrets in each group. Gray shaded regions show the upper and lower limits of detection in the assay. For the same ferrets, titres to A/H3N2 strains are shown in the left column and A/H1N1 strains in the right column. Red dashed lines show times of exposures. Groups A-E correspond to descriptions in Fig 1. Exposure events are as described in Table 1. Symbols above each subplot: star represents infection; syringe represents TIV; and syringe with gray border represents TIV + adjuvant. Symbols are coloured based on their formulation. TIV 1 contained the following influenza A strains: A/Solomon Islands/3/2006 (H1N1) and A/Brisbane/10/2007 (H3N2). TIV 2 contained: A/Solomon Islands/3/2006 (H1N1) and A/Wisconsin/67/2005 (H3N2).

Fig 4. Estimated model parameters. Intervals and points show 95% quantiles and medians respectively. Dashed gray lines show bounds on uniform prior. (i) Estimates for homologous boosting parameter, μ. (ii) Estimates for homologous boost at the end of the initial waning period, $\mu(1 - d)$. (iii) Estimates for duration of initial waning phase, t_s. (iv) Estimates for proportion of initial boost lost during the initial waning phase, d. (v) Estimates for long term waning rate, m. Estimates for TIV 1, TIV 1 + adjuvant and Infection 2 excluded due to lack of identifiability. (vi) Estimates for cross reactivity gradient, σ. Note that this value is fixed at 1 for priming infection (Infection 1), shown by the horizontal dotted line. Values for TIV 2 and TIV 1 + adjuvant excluded due to lack of identifiability.

Fig 5. Estimated cross reactivity profiles by exposure type. Solid black lines shows posterior means; shaded regions show 95% credible intervals. Dashed black lines show antigenic distances and corresponding cross reactive boosts given the strains used here. Note that the y-intercept shows the degree of homologous boosting for that exposure type. Table shows assumed antigenic distances between each strain, with no cross reactivity between subtypes.

Supporting information

Supporting Protocol S1. Details of the full model, model comparison analysis, model fitting and additional sensitivity analyses.

Table S1. Description of model parameters. Summary of parameter definitions and bounds. All bounds relate to lower and upper bounds of the uniform prior distribution used during model fitting.

Table S2. Description of model mechanisms and their potential options.

Table S3. Description of all model variants with δWAIC < 50. Table is ranked by WAIC score, such that the model best supported by WAIC (lowest) is at the

top.

Table S4. Summary of parameter estimates for the best supported model (lowest WAIC score).

Table S5. .csv file containing all posterior distribution estimates for all model variants.

Fig S1. Summary of model mechanisms A: Cross reactive antibody boosting. The degree of boosting decreases as the antigenic distance between the exposure and measured strain increases. Different exposure types may have different gradients; B: Illustrative example of exposure type specific parameter values. Level of homologous boosting may depend on the exposure type. Note that this may also apply to other parameters eg. waning rate; C: Joint effect of exposure boosting and priming infection. Full boosting following a primed exposure is the sum of contributions of the exposure itself and the effect of priming; D: Antigenic seniority mechanism. Parameters ρ_2, ρ_3, ρ_4. Each subsequent exposure elicits a relatively smaller boost compared to the previous exposure; E: titre dependent boosting. Solid black line shows example where $-1 \leq \gamma \leq 1$. Blue dashed lines show boundary conditions. Note that the realized boost does not change when y_i is above y_{switch}.

Fig S2. Observation error matrix. Probability of observing a particular log titre given an underlying true titre. Note that the true titre is a continuous value, whereas observations are discrete. Furthermore, truncation of the distribution at the upper and lower limit of the assay results in an asymmetrical distribution when the true value is at either of these limits. True values outside of these limits will be observed as a value within the assay limits.

Fig S3. Posterior estimates for titre dependent boosting relationship from second best supported model (δWAIC < 5), which included titre dependent boosting. Shaded gray regions shows 95% credible intervals (CI) drawn from the multivariate posterior. Solid black line shows multivariate posterior mean; Dashed gray lines show upper and lower 95% CI for realised antibody boosting from a titre of 12,

given baseline boosting of $\mu = 8$. 95% CI do not exclude no relationship between initial titre at time of exposure and amount of realised boosting, suggesting that titre-dependent boosting was no identifiable here.

Fig S4. Summary of posterior distribution estimates for homologous boosting parameter, μ from models with δWAIC < 75. Points show posterior median; line ranges show 95% credible intervals. Estimates are stratified by exposure type and ordered in order of increasing WAIC. Estimates are coloured according to whether or not cross reactivity was assumed to be a universal parameter or type-specific. Dashed horizontal lines represent uniform prior range. Model codes on x-axis relate to the first letter of each mechanism as described in the table.

Fig S5. Summary of posterior distribution estimates for post-initial waning homologous boosting, $\mu(1-d)$ from models with δWAIC < 75. Points show posterior median; line ranges show 95% credible intervals. Estimates are stratified by exposure type and ordered in order of increasing WAIC. Estimates are coloured according to whether or not cross reactivity was assumed to be a universal parameter or type-specific. Dashed horizontal lines represent uniform prior range. Model codes on x-axis relate to the first letter of each mechanism as described in the table.

Fig S6. Summary of posterior distribution estimates for initial waning phase proportion, d from models with δWAIC < 75. Points show posterior median; line ranges show 95% credible intervals. Estimates are stratified by exposure type and ordered in order of increasing WAIC. Estimates are coloured according to whether or not cross reactivity was assumed to be a universal parameter or type-specific. Dashed horizontal lines represent uniform prior range. Model codes on x-axis relate to the first letter of each mechanism as described in the table.

Fig S7. Summary of posterior distribution estimates for duration of initial waning phase, t_s from models with δWAIC < 75. Points show posterior median; line ranges show 95% credible intervals. Estimates are stratified by exposure type and ordered in order of increasing WAIC. Estimates are coloured according to whether or not cross reactivity was assumed to be a universal parameter or type-specific.

Dashed horizontal lines represent uniform prior range. Model codes on x-axis relate to the first letter of each mechanism as described in the table.

Fig S8. Summary of posterior distribution estimates for long-term waning rate, m from models with δWAIC < 75. Points show posterior median; line ranges show 95% credible intervals. Estimates are stratified by exposure type and ordered in order of increasing WAIC. Estimates are coloured according to whether or not cross reactivity was assumed to be a universal parameter or type-specific. Dashed horizontal lines represent uniform prior range. Model codes on x-axis relate to the first letter of each mechanism as described in the table. Note that the upper y limit is truncated below the upper prior bound for clarity of identifiable estimates.

Fig S9. Summary of posterior distribution estimates for antigenic seniority modifiers, ρ from models with δWAIC < 75. Points show posterior median; line ranges show 95% credible intervals. Estimates are coloured according to whether or not cross reactivity was assumed to be a universal parameter or type-specific. Note that ρ for the first exposure was assumed to be fixed at 1. Estimates are ordered by increasing WAIC. Model codes on x-axis relate to the first letter of each mechanism as described in the table.

Fig S10. Summary of posterior distribution estimates for cross reactivity gradient, σ from models with δWAIC < 75. Points show posterior median; line ranges show 95% credible intervals. Estimates are stratified by exposure type and ordered in order of increasing WAIC. Estimates are coloured according to whether or not cross reactivity was assumed to be a universal parameter or type-specific. Plots are truncated from above at 10 for clarity, but upper prior bound was 100. Red dashed line shows the fixed value of $\sigma = 1$ for priming infection. Blue dashed line shows value above which a homologous boost of μ=5 would give an observed boost of 0 against a strain with an antigenic distance of 1. Model codes on x-axis relate to the first letter of each mechanism as described in the table.

Fig S11. Summary of posterior distribution estimates for priming cross reactivity gradient, β from models with δWAIC < 75. Points show posterior

median; line ranges show 95% credible intervals. Red dashed line shows the fixed value of $\sigma = 1$ for priming infection. Blue dashed line shows value above which a homologous boost of μ=5 would give an observed boost of 0 against a strain with an antigenic distance of 1. Estimates are ordered by increasing WAIC. Model codes on x-axis relate to the first letter of each mechanism as described in the table.

Fig S12. Summary of posterior distribution estimates for titre dependence gradient, γ and titre dependent switch point, y_{switch} from models with δWAIC < 75. Points show posterior median; line ranges show 95% credible intervals. Estimates are coloured according the assumed method of interaction between multiple exposures. Estimates are ordered by increasing WAIC. Model codes on x-axis relate to the first letter of each mechanism as described in the table.

References

1. Kreijtz JHCM, Fouchier RAM, Rimmelzwaan GF. Immune responses to influenza virus infection. Virus Res. 2011;162(1-2):19–30. doi:10.1016/J.VIRUSRES.2011.09.022.

2. Miller E, Hoschler K, Hardelid P, Stanford E, Andrews N, Zambon M. Incidence of 2009 pandemic influenza A H1N1 infection in England: a cross-sectional serological study. Lancet. 2010;375(9720):1100–1108. doi:10.1016/S0140-6736(09)62126-7.

3. Sridhar S, Begom S, Bermingham A, Hoschler K, Adamson W, Carman W, et al. Cellular immune correlates of protection against symptomatic pandemic influenza. Nat Med. 2013;19(10):1305–1312. doi:10.1038/nm.3350.

4. Hobson D, Curry RL, Beare AS, Ward-Gardner A. The role of serum haemagglutination-inhibiting antibody in protection against challenge infection with influenza A2 and B viruses. J Hyg. 1972;70(04):767.

5. Potter CW, Oxford JS. Determinants of immunity to influenza infection in man. Br Med Bull. 1979;35(1):69–75.

6. Bedford T, Riley S, Barr IG, Broor S, Chadha M, Cox NJ, et al. Global circulation patterns of seasonal influenza viruses vary with antigenic drift. Nature. 2015;523(7559):217–220. doi:10.1038/nature14460.

7. Russell CA, Jones TC, Barr IG, Cox NJ, Garten RJ, Gregory V, et al. The Global Circulation of Seasonal Influenza A (H3N2) Viruses. Science. 2008;320(5874).

8. Petrova VN, Russell CA. The evolution of seasonal influenza viruses. Nat Rev Microbiol. 2017;16(1):47–60. doi:10.1038/nrmicro.2017.118.

9. Smith DJ, Forrest S, Ackley DH, Perelson AS. Variable efficacy of repeated annual influenza vaccination. Proc Natl Acad Sci USA. 1999;96(24):14001–14006.

10. Flannery B, Chung JR, Belongia EA, McLean HQ, Gaglani M, Murthy K, et al. Interim Estimates of 2017–18 Seasonal Influenza Vaccine Effectiveness — United States, February 2018. MMWR Morb Mortal Wkly Rep. 2018;67(6):180–185. doi:10.15585/mmwr.mm6706a2.

11. Zost SJ, Parkhouse K, Gumina ME, Kim K, Diaz Perez S, Wilson PC, et al. Contemporary H3N2 influenza viruses have a glycosylation site that alters binding of antibodies elicited by egg-adapted vaccine strains. Proc Natl Acad Sci USA. 2017;114(47):12578–12583. doi:10.1073/pnas.1712377114.

12. Li GM, Chiu C, Wrammert J, McCausland M, Andrews SF, Zheng NY, et al. Pandemic H1N1 influenza vaccine induces a recall response in humans that favors broadly cross-reactive memory B cells. Proc Natl Acad Sci USA. 2012;109(23):9047–52. doi:10.1073/pnas.1118979109.

13. Pebody R, Warburton F, Ellis J, Andrews N, Potts A, Cottrell S, et al. Effectiveness of seasonal influenza vaccine for adults and children in preventing laboratory-confirmed influenza in primary care in the United Kingdom: 2015/16 end-of-season results. Eurosurveillance. 2016;21(38):30348. doi:10.2807/1560-7917.ES.2016.21.38.30348.

14. Kucharski AJ, Lessler J, Read JM, Zhu H, Jiang CQ, Guan Y, et al. Estimating the Life Course of Influenza A(H3N2) Antibody Responses from Cross-Sectional Data. PLoS Biol. 2015;13(3):1–16. doi:10.1371/journal.pbio.1002082.

15. Andrews SF, Huang Y, Kaur K, Popova LI, Ho IY, Pauli NT, et al. Immune history profoundly affects broadly protective B cell responses to influenza. Sci Transl Med. 2015;7(316):316ra192–316ra192. doi:10.1126/scitranslmed.aad0522.

16. Quiñones-Parra SM, Clemens EB, Wang Z, Croom HA, Kedzierski L, McVernon J, et al. A Role of Influenza Virus Exposure History in Determining Pandemic Susceptibility and CD8+ T Cell Responses. J Virol. 2016;90(15):6936–6947. doi:10.1128/JVI.00349-16.

17. Fonville JM, Wilks SH, James SL, Fox A, Ventresca M, Aban M, et al. Antibody landscapes after influenza virus infection or vaccination. Science. 2014 Nov 21;346(6212):996-1000. doi: 10.1126/science.1256427.

18. Kucharski AJ, Lessler J, Cummings DAT, Riley S. Timescales of influenza A/H3N2 antibody dynamics. PLoS Biol. 2018;16(8):e2004974. doi:10.1371/journal.pbio.2004974.

19. Wrammert J, Smith K, Miller J, Langley WA, Kokko K, Larsen C, et al. Rapid cloning of high-affinity human monoclonal antibodies against influenza virus. Nature. 2008;453(7195):667–671. doi:10.1038/nature06890.

20. Cobey S, Hensley SE. Immune history and influenza virus susceptibility. Curr Opin Virol. 2017;doi:10.1016/j.coviro.2016.12.004.

21. Skowronski DM, Chambers C, De Serres G, Sabaiduc S, Winter AL, Dickinson JA, et al. Serial Vaccination and the Antigenic Distance Hypothesis: Effects on Influenza Vaccine Effectiveness During A(H3N2) Epidemics in Canada, 2010-2011 to 2014-2015. J Infect Dis. 2017;215(7):1059–1099.

22. Woolthuis RG, Wallinga J, van Boven M. Variation in loss of immunity shapes influenza epidemics and the impact of vaccination. BMC Infect Dis. 2017;17(1):632. doi:10.1186/s12879-017-2716-y.

23. Kim JH, Skountzou I, Compans R, Jacob J. Original Antigenic Sin Responses to Influenza Viruses. J Immunol. 2009;183(5):3294–3301. doi:10.4049/jimmunol.0900398.

24. Gostic KM, Ambrose M, Worobey M, Lloyd-Smith JO. Potent protection against H5N1 and H7N9 influenza via childhood hemagglutinin imprinting. Science. 2016;354(6313).

25. Lessler J, Riley S, Read JM, Wang S, Zhu H, Smith GJD, et al. Evidence for antigenic seniority in influenza A (H3N2) antibody responses in southern China. PLoS Pathog. 2012;8(7):e1002802. doi:10.1371/journal.ppat.1002802.

26. Lee HY, Topham DJ, Park SY, Hollenbaugh J, Treanor J, Mosmann TR, et al. Simulation and prediction of the adaptive immune response to influenza A virus infection. J Virol. 2009;83(14):7151–65. doi:10.1128/JVI.00098-09.

27. Ranjeva S, Subramanian R, Fang VJ, Leung GM, Ip DKM, Perera RAPM, et al. Age-specific differences in the dynamics of protective immunity to influenza. bioRxiv. 2018; p. 330720. doi:10.1101/330720.

28. Zhao X, Ning Y, Chen MIC, Cook AR. Individual and Population Trajectories of Influenza Antibody Titers Over Multiple Seasons in a Tropical Country. Am J Epidemiol. 2018;187(1):135–143. doi:10.1093/aje/kwx201.

29. Laurie KL, Carolan La, Middleton D, Lowther S, Kelso A, Barr IG. Multiple infections with seasonal influenza A virus induce cross-protective immunity against A(H1N1) pandemic influenza virus in a ferret model. J Infect Dis. 2010;202(7):1011–1020. doi:10.1086/656188.

30. Maher JA, Ms JD. The Ferret : An Animal Model to Study Influenza Virus. Lab Anim (NY). 2004;33(9):50–53. doi:10.1038/laban1004-50.

31. McLaren C, Potter CW. Immunity to influenza in ferrets. VII. Effect of previous infection with heterotypic and heterologous influenza viruses on the response of ferrets to inactivated influenza virus vaccines. J Hyg. 1974;72(1):91–100. doi:10.1017/S0022172400023251.

32. Kim JH, Liepkalns J, Reber AJ, Lu X, Music N, Jacob J, et al. Prior infection with influenza virus but not vaccination leaves a long-term immunological imprint that intensifies the protective efficacy of antigenically drifted vaccine strains. Vaccine. 2016;34(4):495–502. doi:10.1016/j.vaccine.2015.11.077.

33. Kreijtz JHCM, Bodewes R, van Amerongen G, Kuiken T, Fouchier RAM, Osterhaus ADMEDME, et al. Primary influenza A virus infection induces cross-protective immunity against a lethal infection with a heterosubtypic virus strain in mice. Vaccine. 2007;25(4):612–620. doi:10.1016/j.vaccine.2006.08.036.

34. Miao H, Hollenbaugh JA, Zand MS, Holden-Wiltse J, Mosmann TR, Perelson AS, et al. Quantifying the early immune response and adaptive immune response kinetics in mice infected with influenza A virus. J Virol. 2010;84(13):6687–98. doi:10.1128/JVI.00266-10.

35. Kosikova M, Li L, Radvak P, Ye Z, Wan XF, Xie H. Imprinting of Repeated Influenza A/H3 Exposures on Antibody Quantity and Antibody Quality: Implications on Seasonal Vaccine Strain Selection and Vaccine Performance. Clin Infect Dis. 2018;doi:10.1093/cid/ciy327.

36. Fonville JM, Fraaij PLA, de Mutsert G, Wilks SH, van Beek R, Fouchier RAM, et al. Antigenic Maps of Influenza A(H3N2) Produced With Human Antisera Obtained After Primary Infection. J Infect Dis. 2016;213(1):31–8. doi:10.1093/infdis/jiv367.

37. Goji N, Nolan C, Hill H, Wolff M, Noah D, Williams T, et al. Immune Responses of Healthy Subjects to a Single Dose of Intramuscular Inactivated Influenza A/Vietnam/1203/2004 (H5N1) Vaccine after Priming with an Antigenic Variant. J Infect Dis. 2008;198(5):635–641. doi:10.1086/590916.

38. Rudenko L, Naykhin A, Donina S, Korenkov D, Petukhova G, Isakova-Sivak I, et al. Assessment of immune responses to H5N1 inactivated influenza vaccine among individuals previously primed with H5N2 live attenuated influenza vaccine. Hum Vaccin Immunother. 2015;11(12):2839–2848.

39. Bodewes R, Kreijtz JHCM, Geelhoed-Mieras MM, van Amerongen G, Verburgh RJ, van Trierum SE, et al. Vaccination against seasonal influenza A/H3N2 virus

reduces the induction of heterosubtypic immunity against influenza A/H5N1 virus infection in ferrets. J Virol. 2011;85(6):2695–702. doi:10.1128/JVI.02371-10.

40. van den Brand JMA, Kreijtz JHCM, Bodewes R, Stittelaar KJ, van Amerongen G, Kuiken T, et al. Efficacy of vaccination with different combinations of MF59-adjuvanted and nonadjuvanted seasonal and pandemic influenza vaccines against pandemic H1N1 (2009) influenza virus infection in ferrets. J Virol. 2011;85(6):2851–8. doi:10.1128/JVI.01939-10.

41. Khurana S, Chearwae W, Castellino F, Manischewitz J, King LR, Honorkiewicz A, et al. Vaccines with MF59 adjuvant expand the antibody repertoire to target protective sites of pandemic avian H5N1 influenza virus. Sci Transl Med. 2010;2(15):15ra5. doi:10.1126/scitranslmed.3000624.

42. Wright PF, Sannella E, Shi JR, Zhu Y, Ikizler MR, Edwards KM. Antibody Responses After Inactivated Influenza Vaccine in Young Children. Pediatr Infect Dis J. 2008;27(11):1004–1008. doi:10.1097/INF.0b013e31817d53c5.

43. Frank AL, Taber LH, Glezen WP, Paredes A, Couch RB. Reinfection with Influenza A (H3N2) Virus in Young Children and Their Families. J Infect Dis. 1979;140(6):829–833. doi:10.1093/infdis/140.6.829.

44. Jacobson RM, Grill DE, Oberg AL, Tosh PK, Ovsyannikova IG, Poland GA. Profiles of influenza A/H1N1 vaccine response using hemagglutination-inhibition titers. Hum Vaccin Immunother. 2015;11(4):961–969. doi:10.1080/21645515.2015.1011990.

45. Freeman G, Pereram RAPM, Ngan E, Fang VJ, Cauchemez S, Ip DKM, et al. Quantifying homologous and heterologous antibody titre rises after influenza virus infection. Epidemiol Infect. 2016;144(11):2306–2316. doi:10.1017/S0950268816000583.

46. Knudsen NPH, Olsen A, Buonsanti C, Follmann F, Zhang Y, Coler RN, et al. Different human vaccine adjuvants promote distinct antigen-independent immunological signatures tailored to different pathogens. Sci Rep. 2016;6:19570. doi:10.1038/srep19570.

47. Hoft DF, Lottenbach KR, Blazevic A, Turan A, Blevins TP, Pacatte TP, et al. Comparisons of the Humoral and Cellular Immune Responses Induced by Live Attenuated Influenza Vaccine and Inactivated Influenza Vaccine in Adults. Clin Vaccine Immunol. 2017;24(1). pii: e00414-16. doi: 10.1128/CVI.00414-16.

48. Basha S, Hazenfeld S, Brady RC, Subbramanian RA. Comparison of antibody and T-cell responses elicited by licensed inactivated- and live-attenuated influenza vaccines against H3N2 hemagglutinin. Hum Immunol. 2011;72(6):463–469. doi:10.1016/j.humimm.2011.03.001.

49. Reber A, Adrian R, Jacqueline K, Katz J. Immunological assessment of influenza vaccines and immune correlates of protection. Expert Rev Vaccines. 2013;12(5):519–36. doi:10.1586/erv.13.35.

50. Dormitzer PR, Galli G, Castellino F, Golding H, Khurana S, Del Giudice G, et al. Influenza vaccine immunology. Immunol Rev. 2011;239(1):167–177. doi:10.1111/j.1600-065X.2010.00974.x.

51. Coudeville L, Bailleux F, Riche B, Megas F, Andre P, Ecochard R. Relationship between haemagglutination-inhibiting antibody titres and clinical protection against influenza: development and application of a bayesian random-effects model. BMC Med Res Methodol. 2010;10:18. doi:10.1186/1471-2288-10-18.

52. Belongia EA, Sundaram ME, McClure DL, Meece JK, Ferdinands J, VanWormer JJ. Waning vaccine protection against influenza A (H3N2) illness in children and older adults during a single season. Vaccine. 2015;33(1):246–251. doi:10.1016/j.vaccine.2014.06.052.

53. Ferdinands JM, Fry AM, Reynolds S, Petrie J, Flannery B, Jackson ML, et al. Intraseason waning of influenza vaccine protection: Evidence from the US Influenza Vaccine Effectiveness Network, 2011-12 through 2014-15. Clin Infect Dis. 2017;64(5):544–550. doi: 10.1093/cid/ciw816.

54. Mugitani A, Ito K, Irie S, Eto T, Ishibashi M, Ohfuji S, et al. Immunogenicity of the Trivalent Inactivated Influenza Vaccine in Young Children Less than 4 Years of Age, with a Focus on Age and Baseline Antibodies. Clin Vaccine Immunol. 2014;21(9):1253–1260. doi:10.1128/CVI.00200-14.

55. Mosterín Höpping A, McElhaney J, Fonville JM, Powers DC, Beyer WEP, Smith DJ, et al. The confounded effects of age and exposure history in response to influenza vaccination. Vaccine. 2016;34(4):540–546. doi:10.1016/j.vaccine.2015.11.058.

56. Allen JD, Owino SO, Carter DM, Crevar CJ, Reese VA, Fox CB, et al. Broadened immunity and protective responses with emulsion-adjuvanted H5 COBRA-VLP vaccines. Vaccine. 2017;35(38):5209–5216. doi:10.1016/J.VACCINE.2017.07.107.

57. Forrest HL, Khalenkov AM, Govorkova EA, Kim JK, Del Giudice G, Webster RG. Single- and multiple-clade influenza A H5N1 vaccines induce cross protection in ferrets. Vaccine. 2009;27(31):4187–4195. doi:10.1016/j.vaccine.2009.04.050.

58. Jackson LA, Campbell JD, Frey SE, Edwards KM, Keitel WA, Kotloff KL, et al. Effect of Varying Doses of a Monovalent H7N9 Influenza Vaccine With and Without AS03 and MF59 Adjuvants on Immune Response: A Randomized Clinical Trial. JAMA. 2015;314(3):237–246. doi: 10.1001/jama.2015.7916.

59. Shoenfeld Y, Agmon-Levin N. 'ASIA' – Autoimmune/inflammatory syndrome induced by adjuvants. J Autoimmun. 2011;36(1):4–8. doi: 10.1016/j.jaut.2010.07.003.

60. Gupta RK, Relyveld EH, Lindblad EB, Bizzini B, Ben-Efraim S, Gupta CK. Adjuvants–a balance between toxicity and adjuvanticity. Vaccine. 1993;11(3):293–306.

61. Galli G, Hancock K, Hoschler K, DeVos J, Praus M, Bardelli M, et al. Fast rise of broadly cross-reactive antibodies after boosting long-lived human memory B cells primed by an MF59 adjuvanted prepandemic vaccine. Proc Natl Acad Sci USA. 2009;106(19):7962–7967. doi:10.1073/pnas.0903181106.

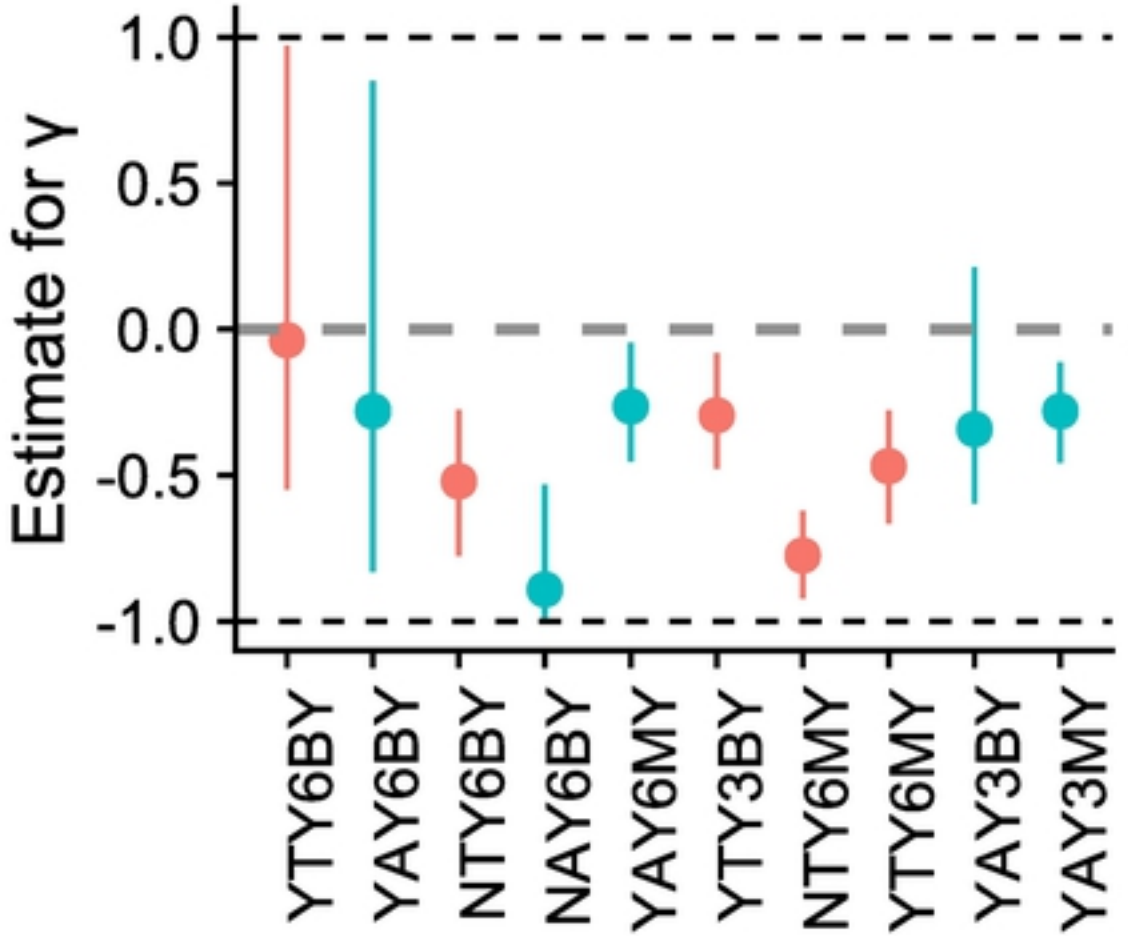

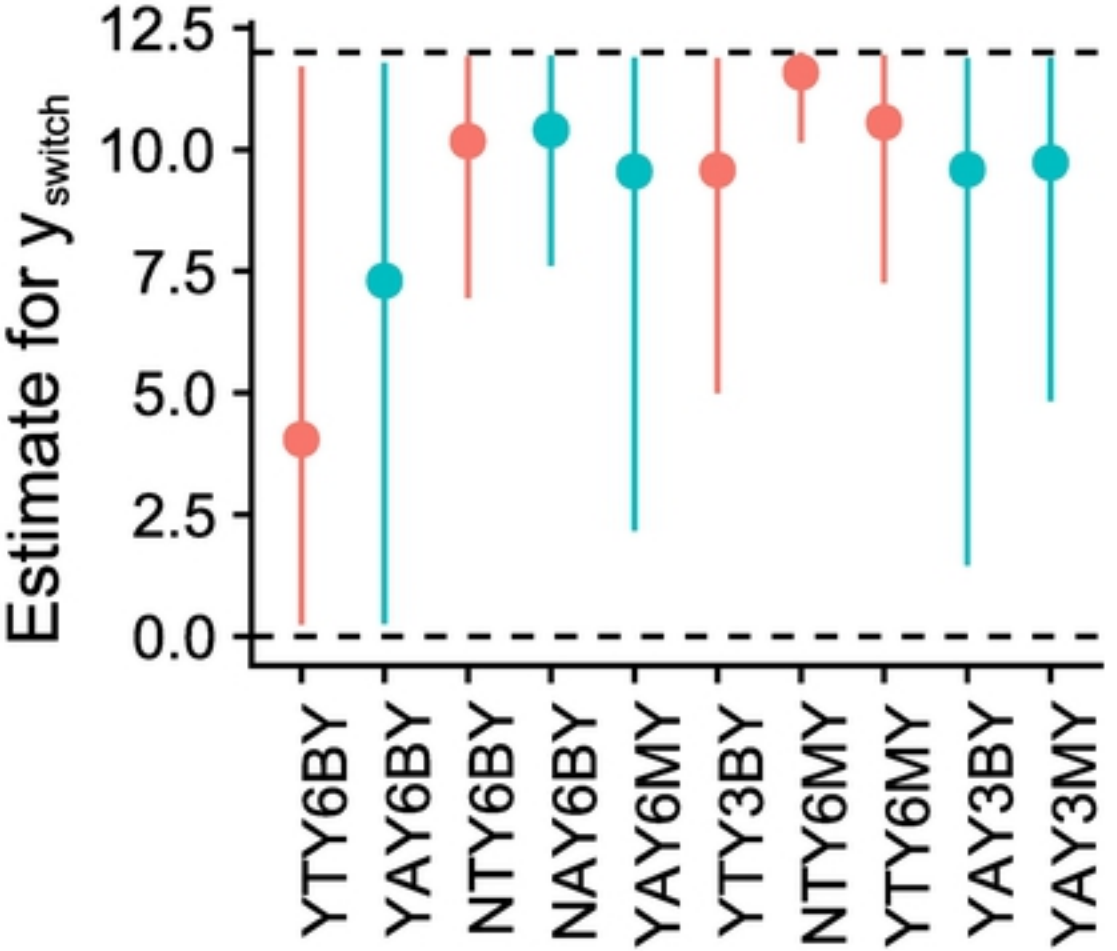

Cross Reactivity

Universal

Type specific

Mechanism	Antigenic seniority	Cross reactivity	Priming	Typed exposures	Waning	Titre dependent boosting
Option 1	Yes	Type specific	Yes	3types	Biphasic	Yes
Option 2	No	All	No	6types	Monophasic	No

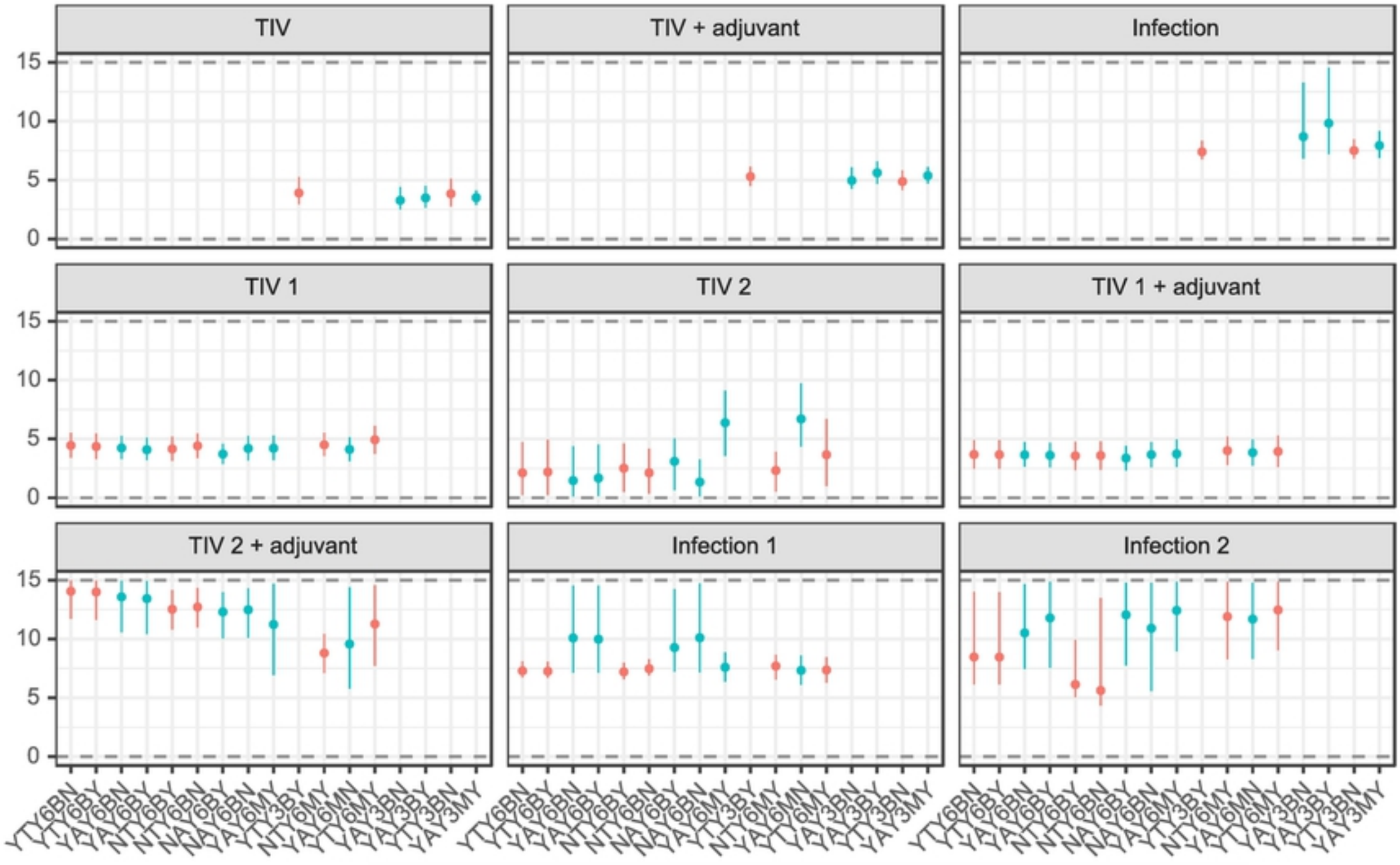

Cross Reactivity

Universal

Type specific

Mechanism	Antigenic seniority	Cross reactivity	Priming	Typed exposures	Waning	Titre dependent boosting
Option 1	Yes	Type specific	Yes	3types	Biphasic	Yes
Option 2	No	All	No	6types	Monophasic	No

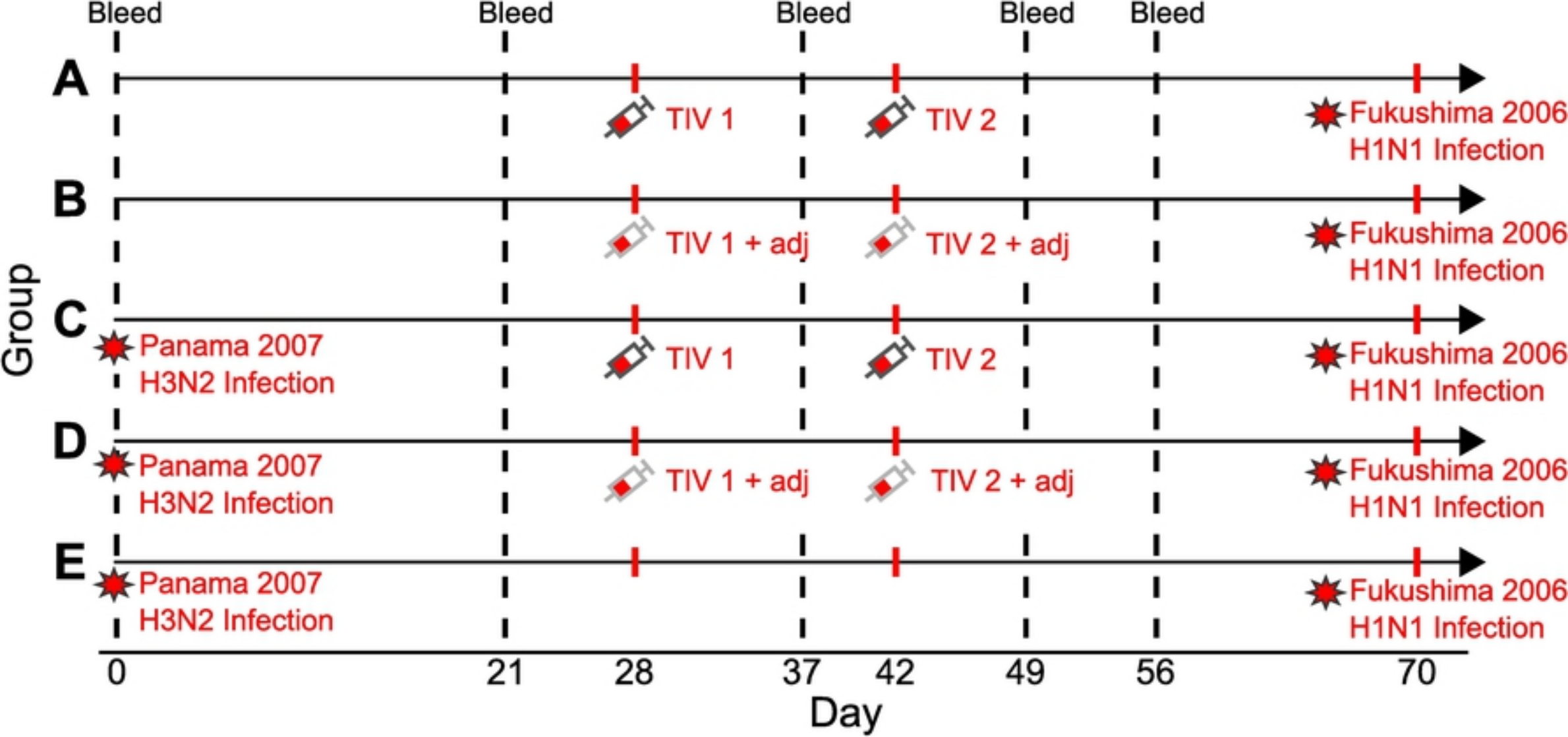
Bleed
Bleed
Bleed
Bleed
Bleed
A
TIV 1
TIV 2
Fukushima 2006
H1N1 Infection
B
TIV 1 + adj
TIV 2 + adj
Fukushima 2006
H1N1 Infection
C
Panama 2007
H3N2 Infection
TIV 1
TIV 2
Fukushima 2006
H1N1 Infection
D
Panama 2007
H3N2 Infection
TIV 1 + adj
TIV 2 + adj
Fukushima 2006
H1N1 Infection
E
Panama 2007
H3N2 Infection
Fukushima 2006
H1N1 Infection
Group
0
21
28
37
42
49
56
70
Day

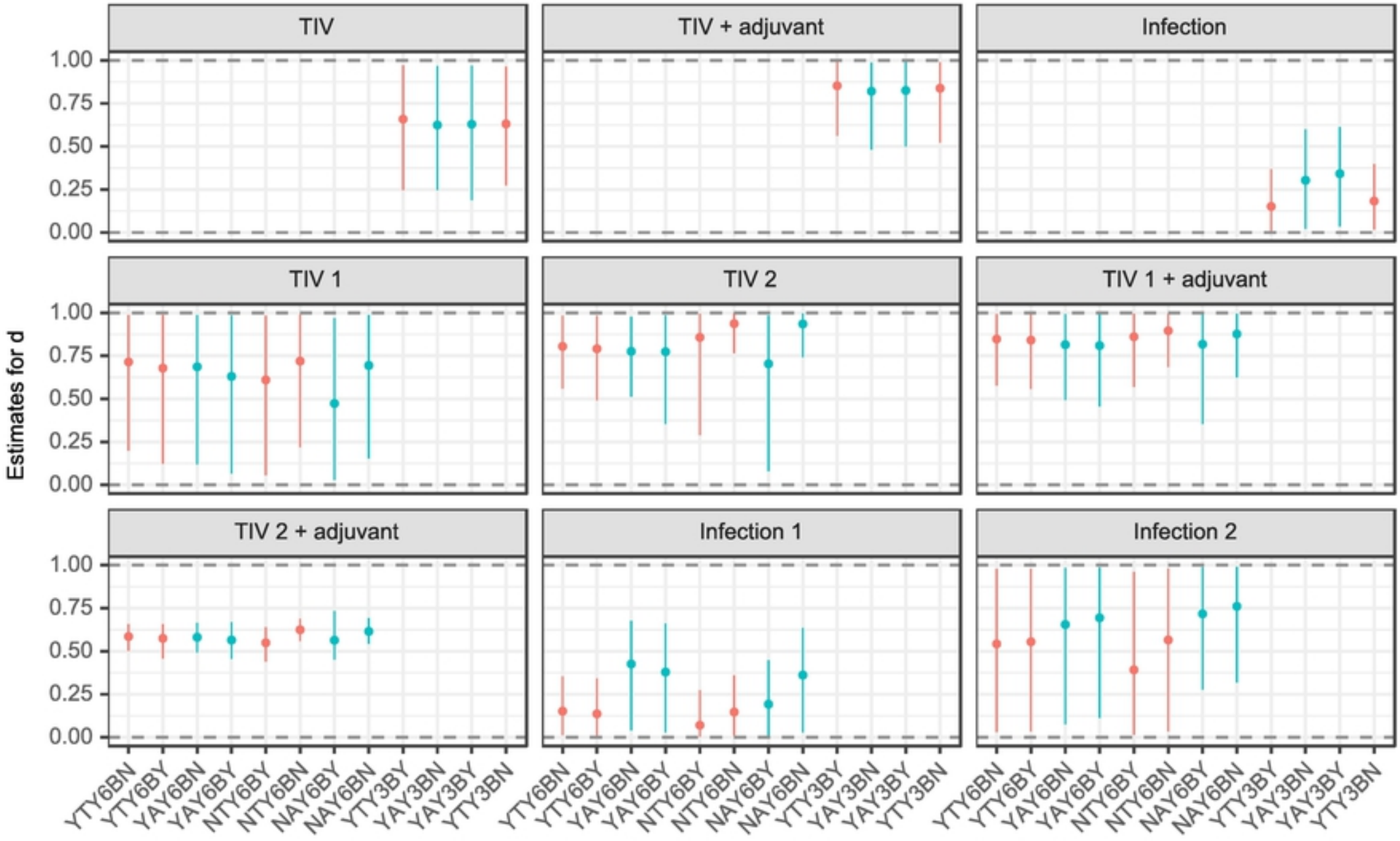

Mechanism	Antigenic seniority	Cross reactivity	Priming	Typed exposures	Waning	Titre dependent boosting
Option 1	Yes	Type specific	Yes	3types	Biphasic	Yes
Option 2	No	All	No	6types	Monophasic	No

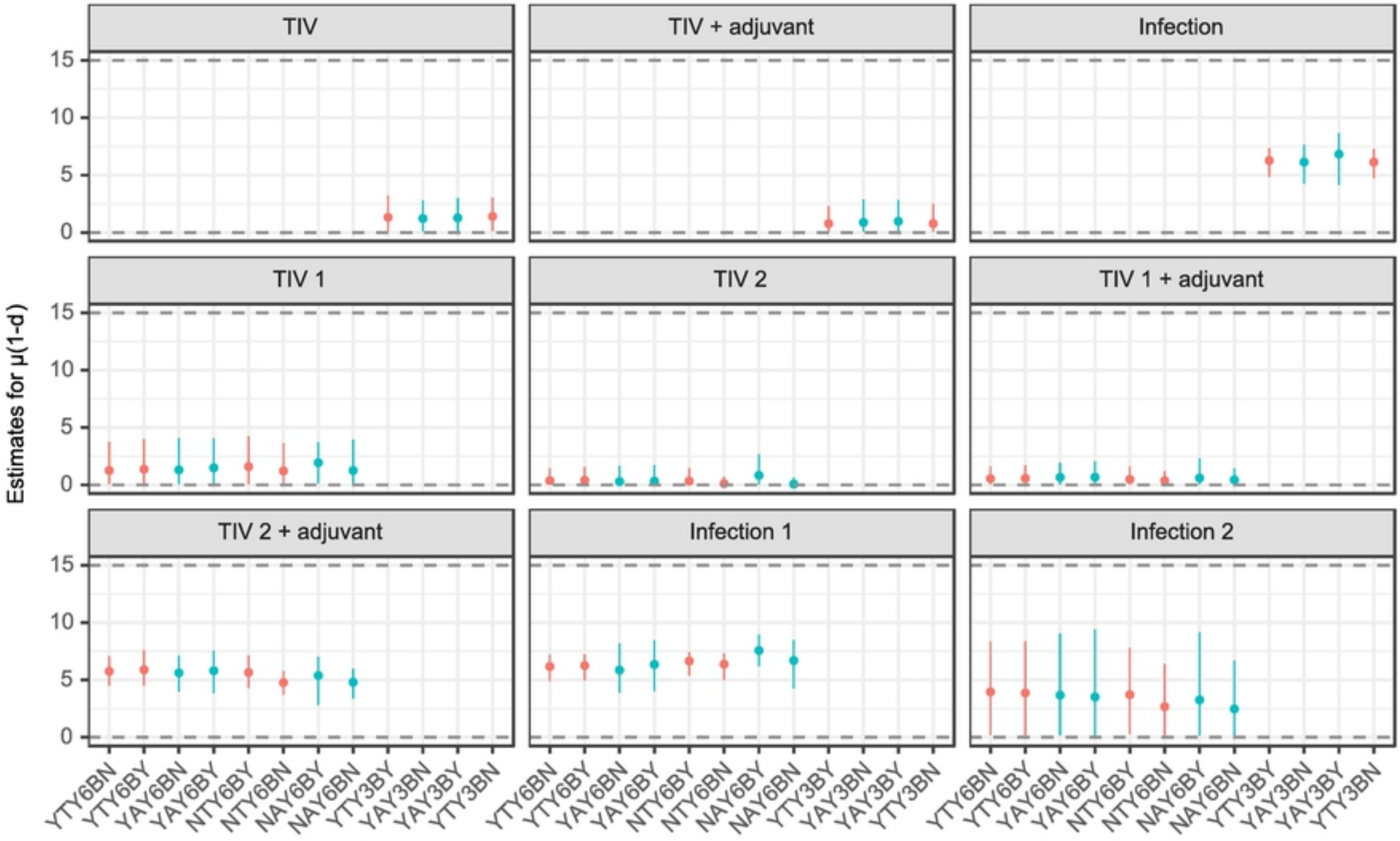

Mechanism	Antigenic seniority	Cross reactivity	Priming	Typed exposures	Waning	Titre dependent boosting
Option 1	Yes	Type specific	Yes	3types	Biphasic	Yes
Option 2	No	All	No	6types	Monophasic	No

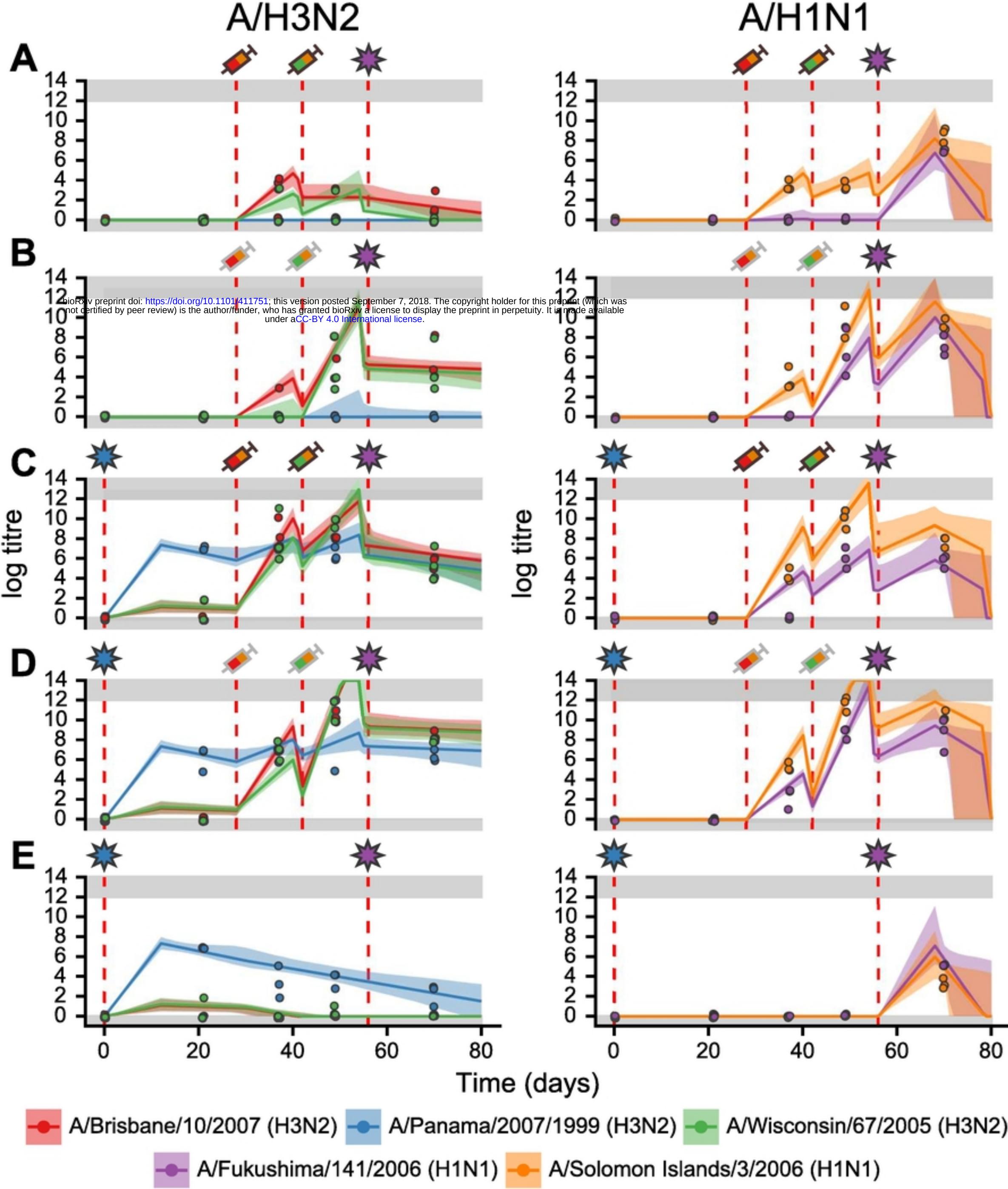

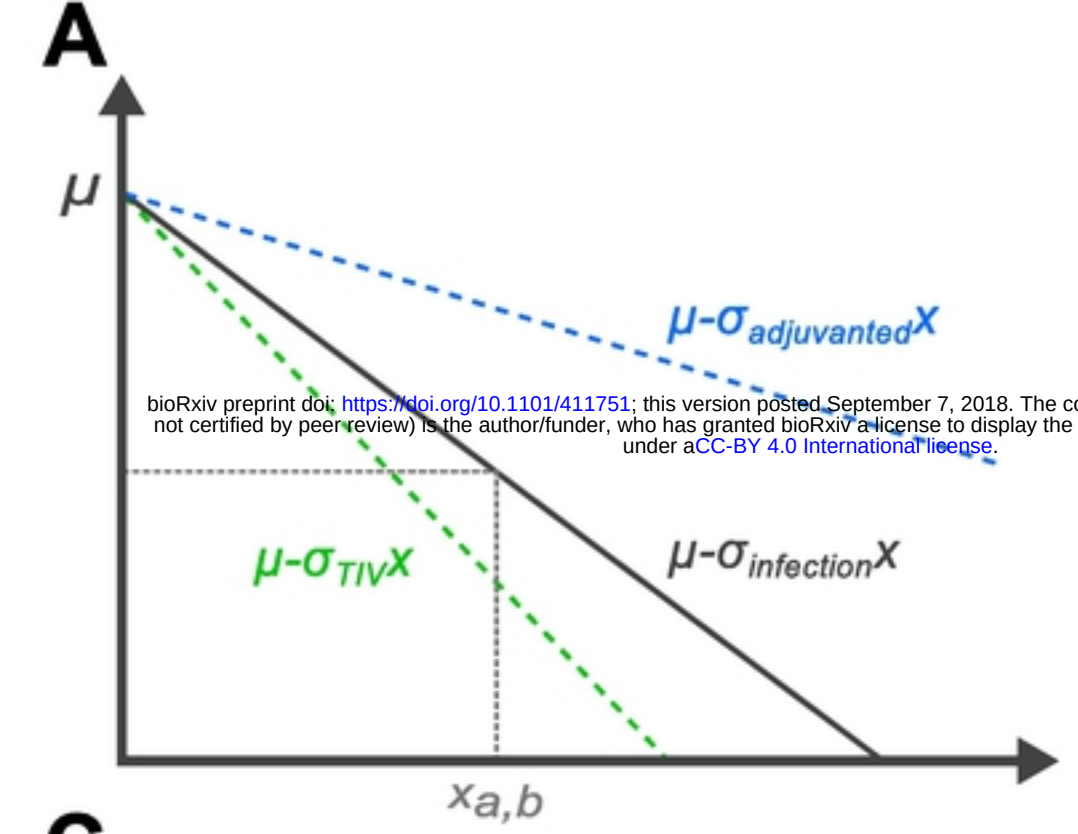

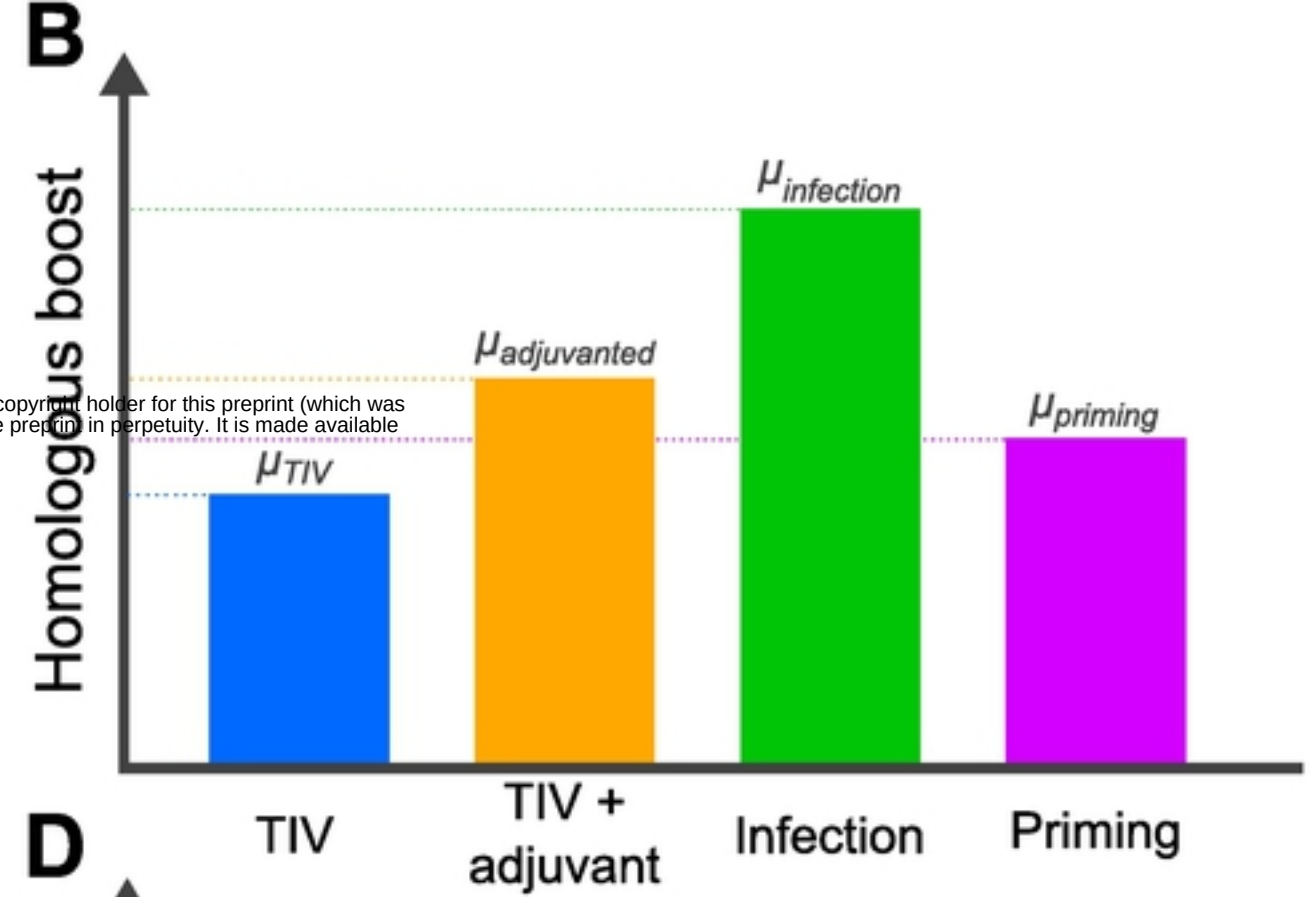

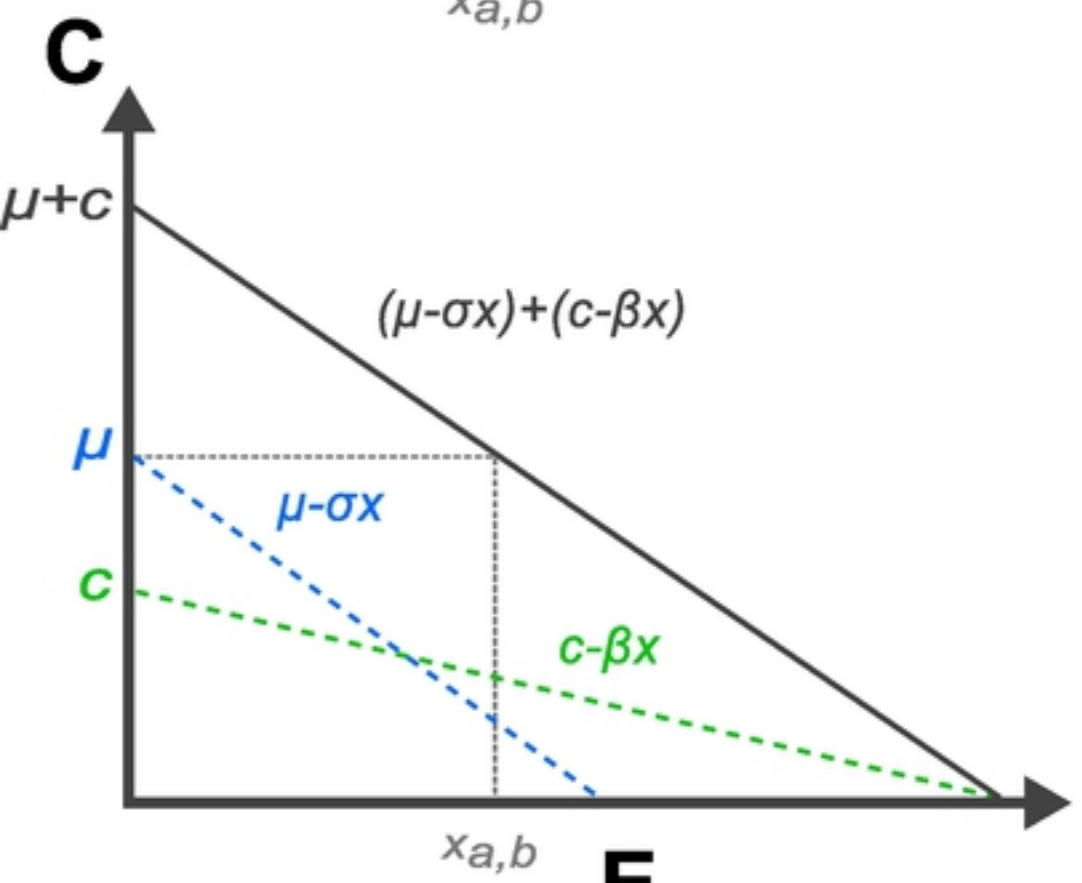

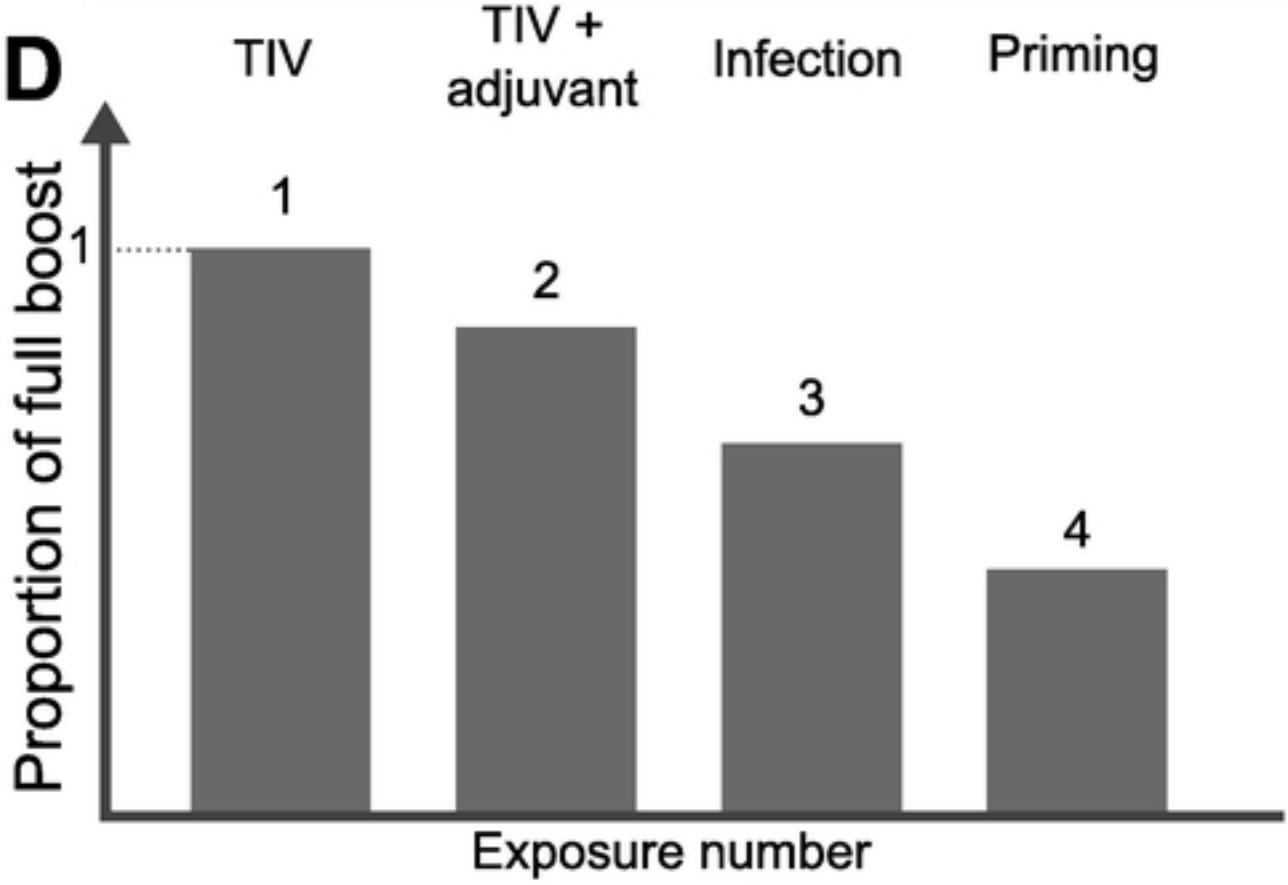

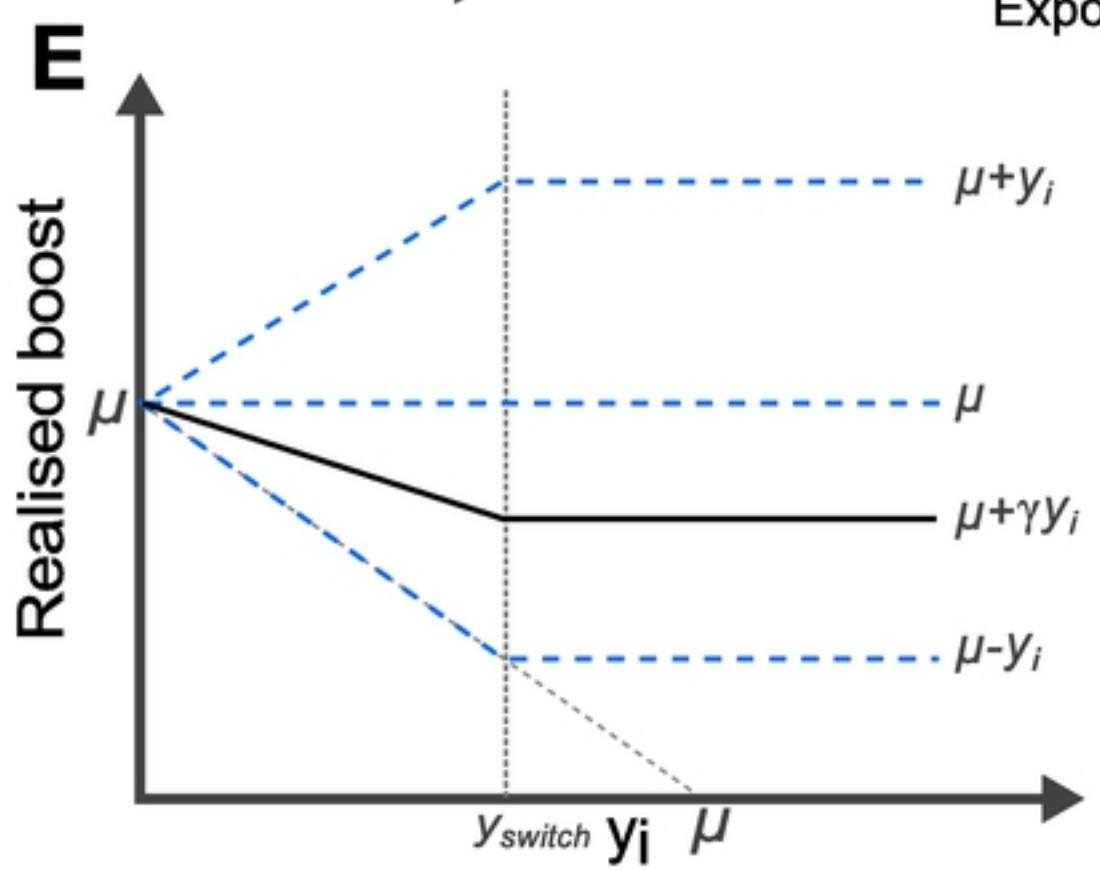

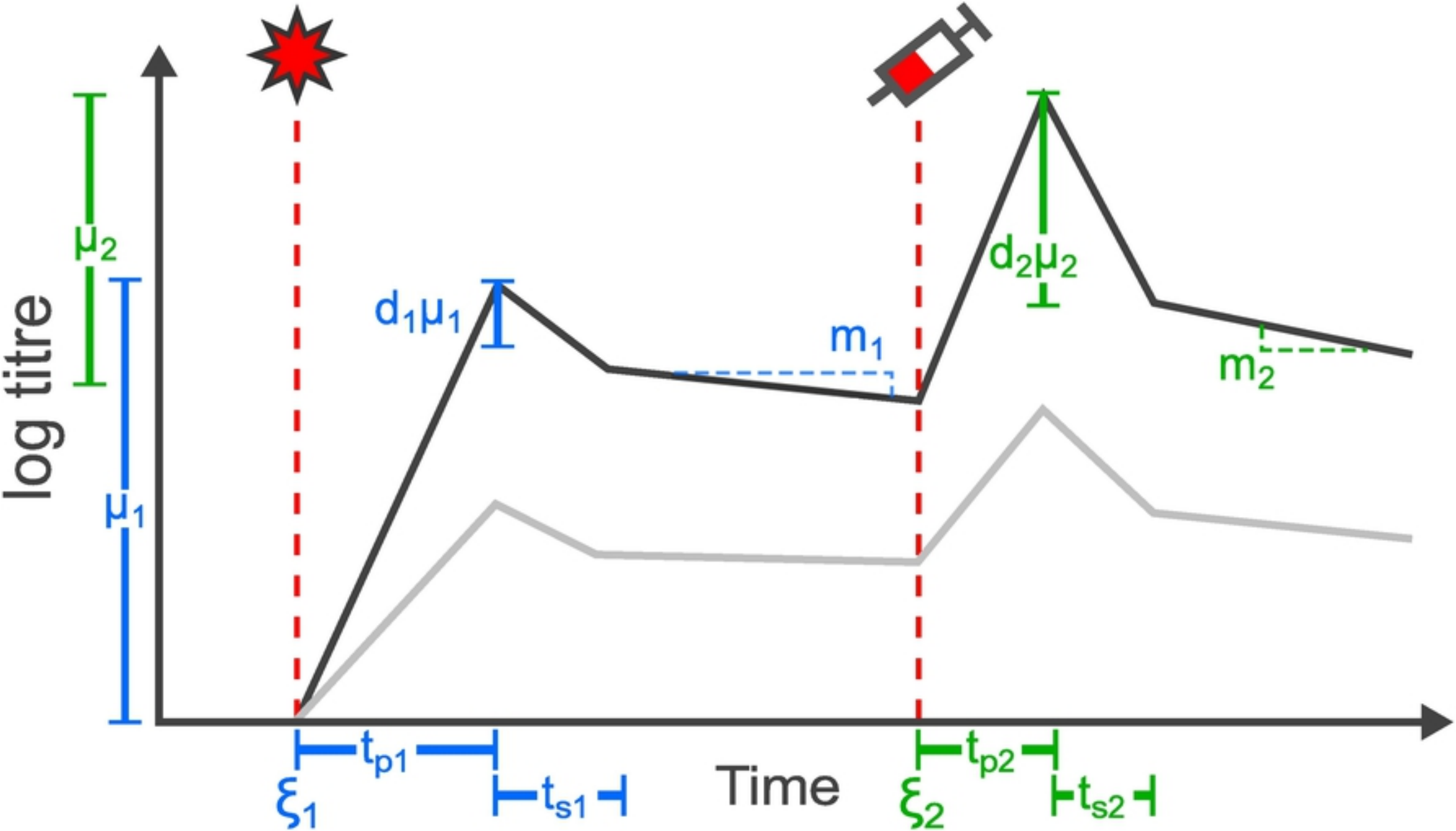
log titre
Time
μ_2
μ_1
$d_1\mu_1$
m_1
$d_2\mu_2$
m_2
t_{p1}
t_{s1}
ξ_1
t_{p2}
t_{s2}
ξ_2

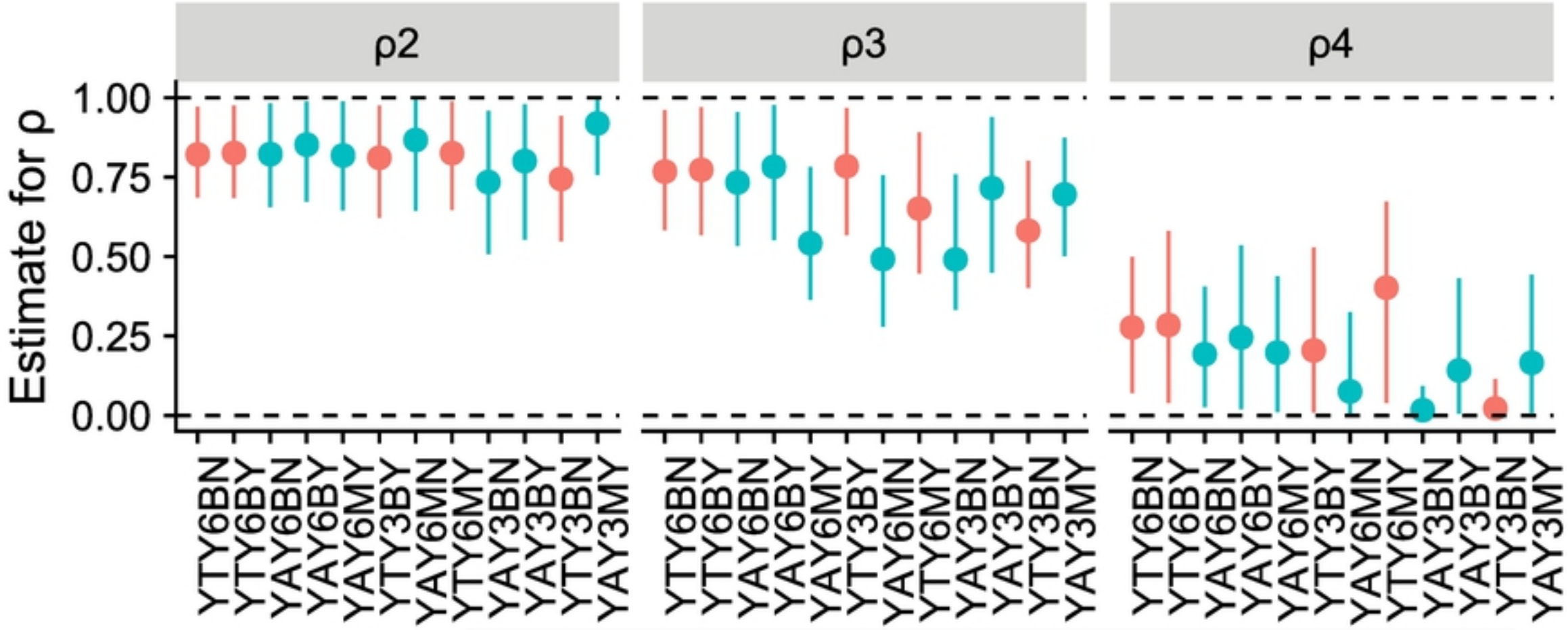

Cross Reactivity

- Universal
- Type specific

Mechanism	Antigenic seniority	Cross reactivity	Priming	Typed exposures	Waning	Titre dependent boosting
Option 1	Yes	Type specific	Yes	3types	Biphasic	Yes
Option 2	No	All	No	6types	Monophasic	No

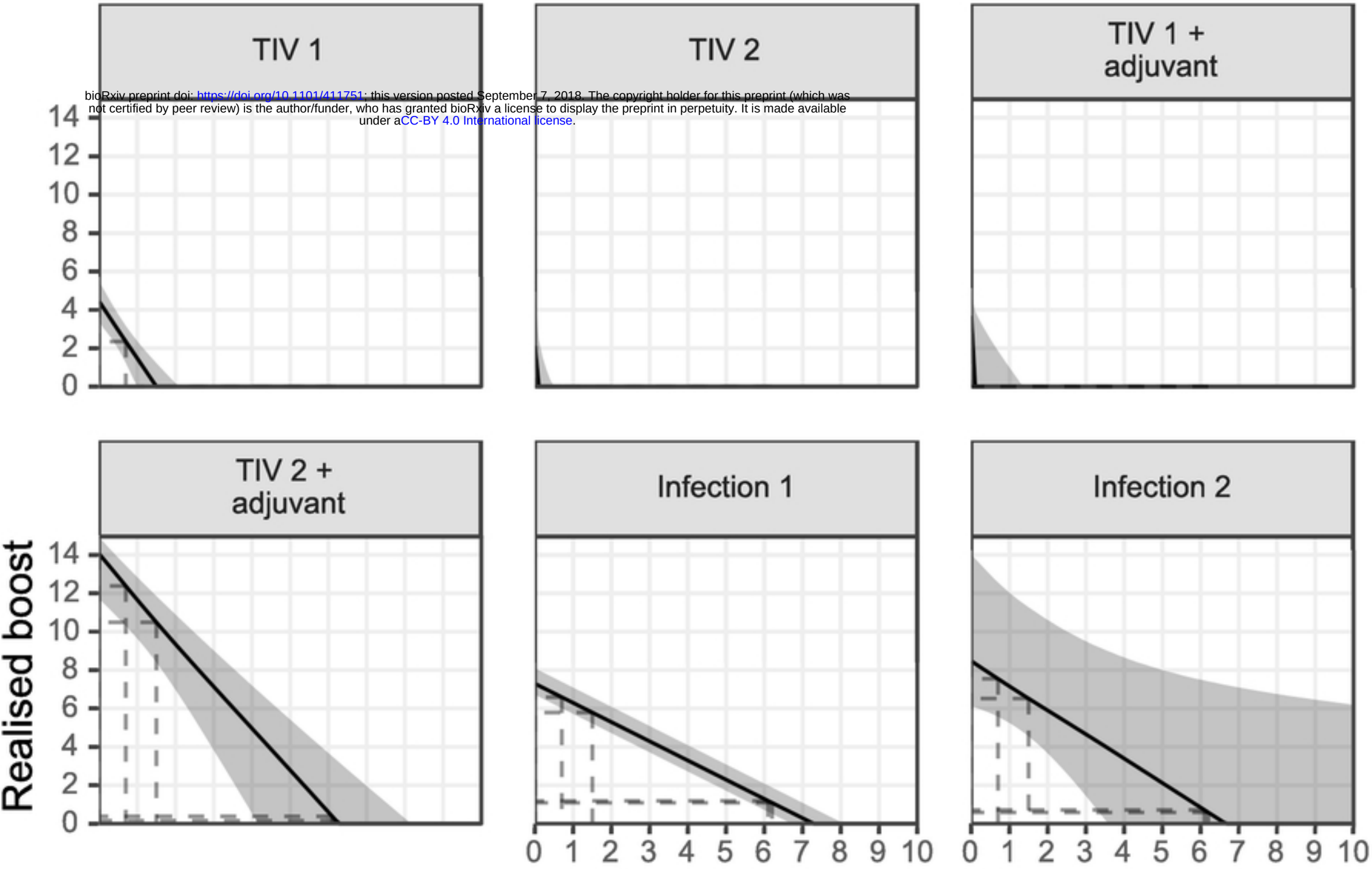

		1)	2)	3)	4)	5)
H3N2	1) A/Brisbane/10/2007	0.00	0.70	6.23	NA	NA
	2) A/Wisconsin/68/2005	0.70	0.00	6.13	NA	NA
	3) A/Panama/2007/1999	6.23	6.13	0.00	NA	NA
H1N1	4) A/Fukushima/141/2006	NA	NA	NA	0.00	1.55
	5) A/Solomon Islands/3/2006	NA	NA	NA	1.55	0.00

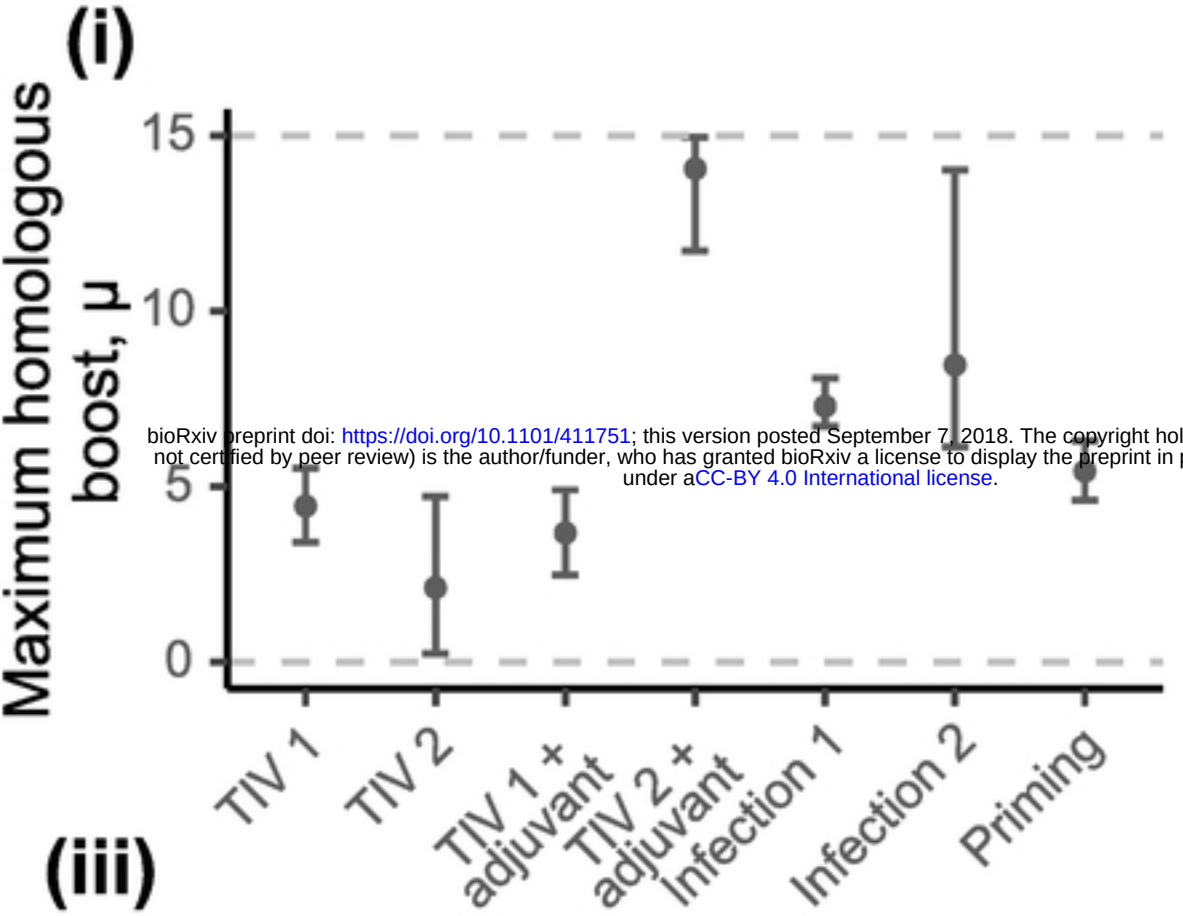

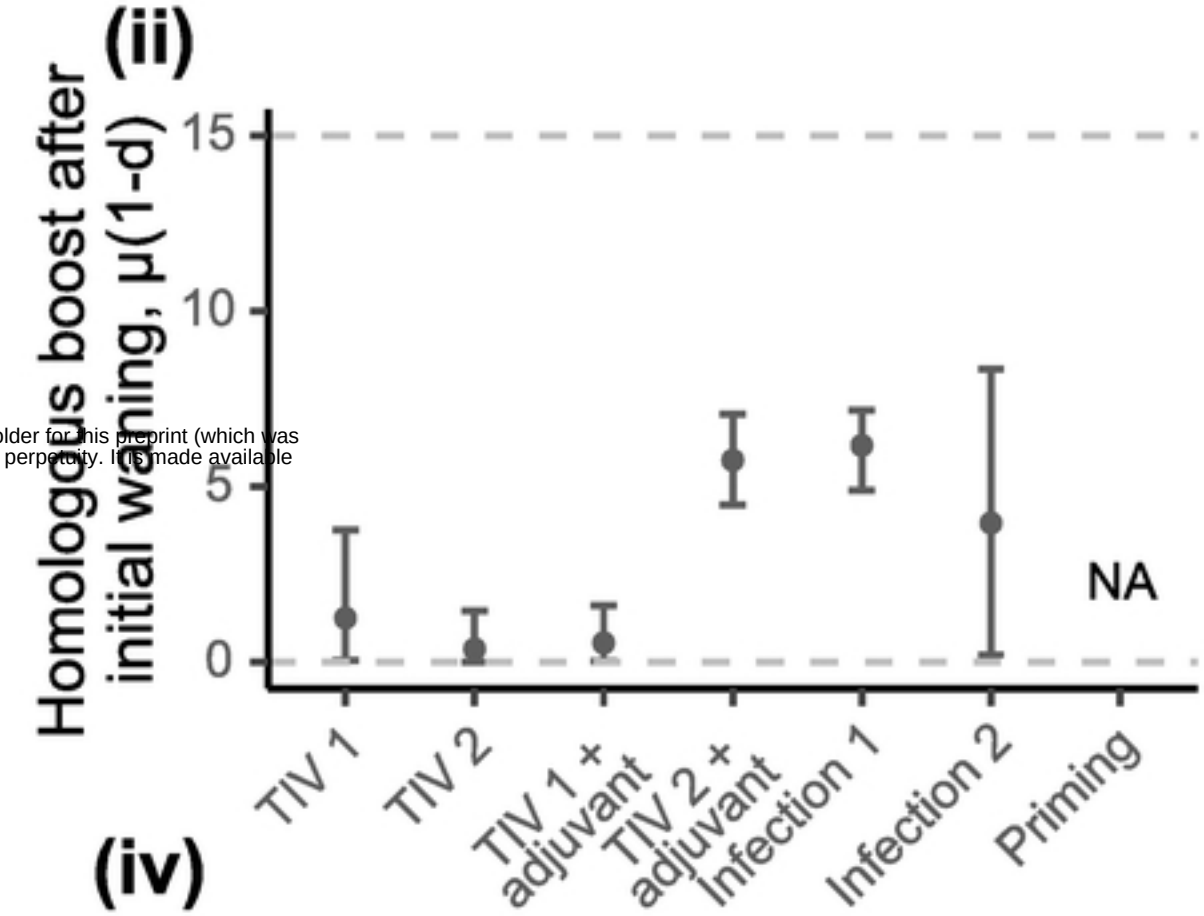

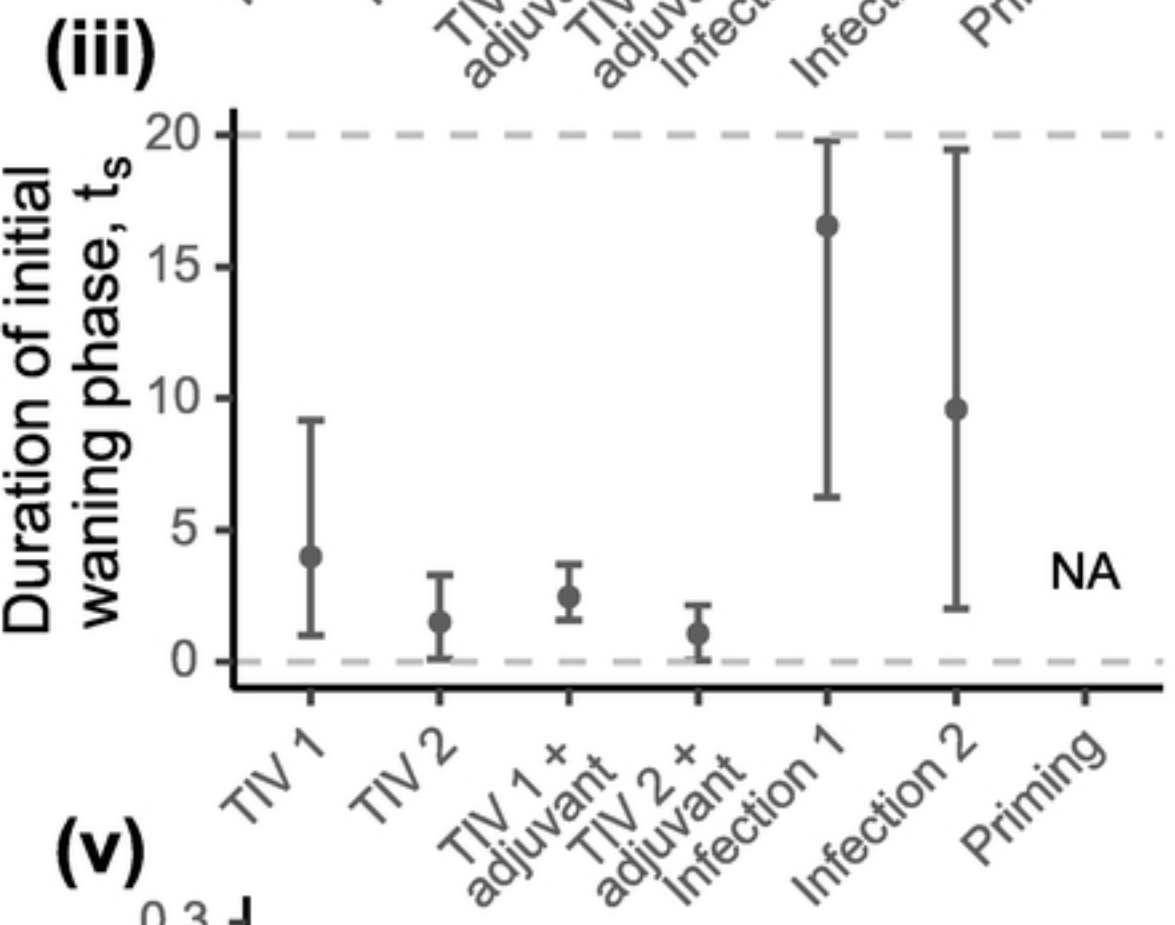

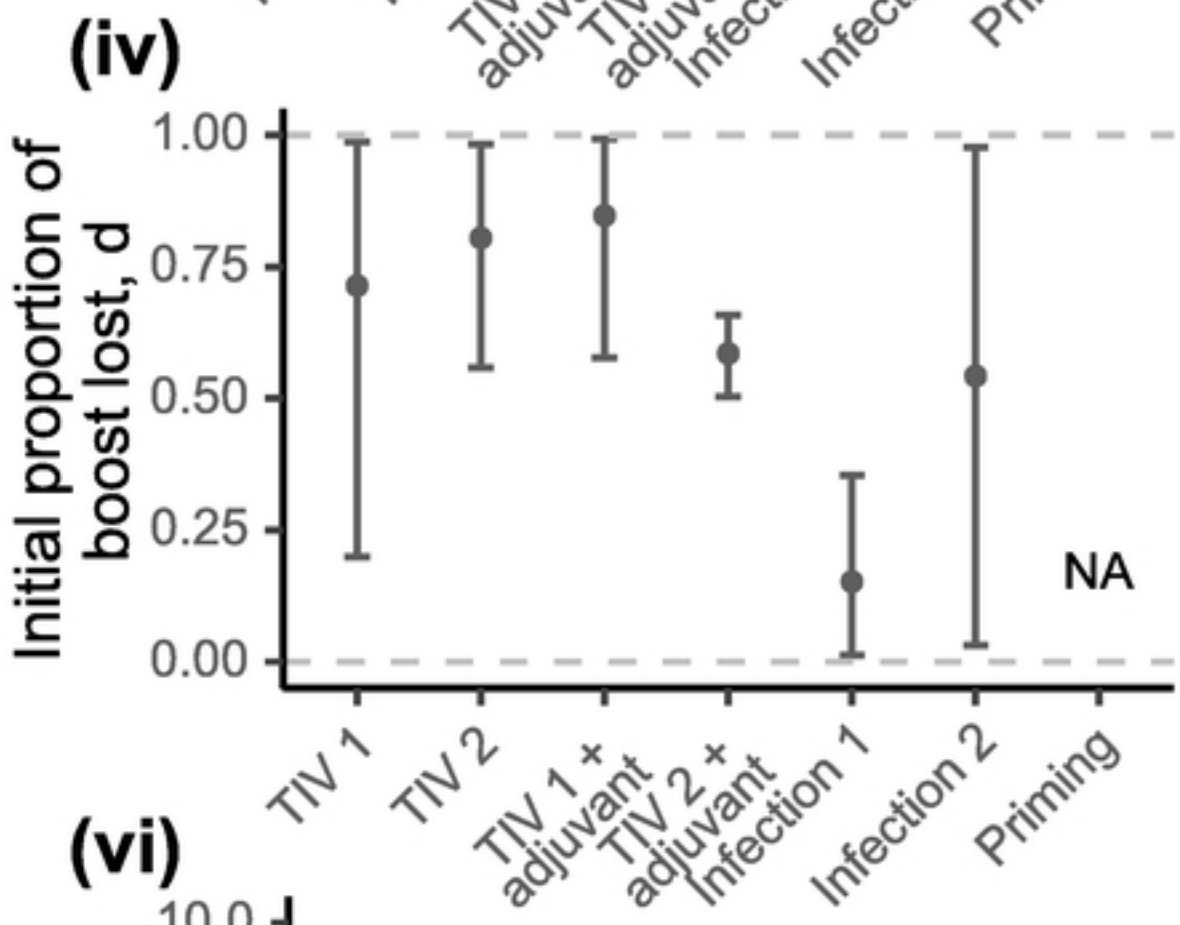

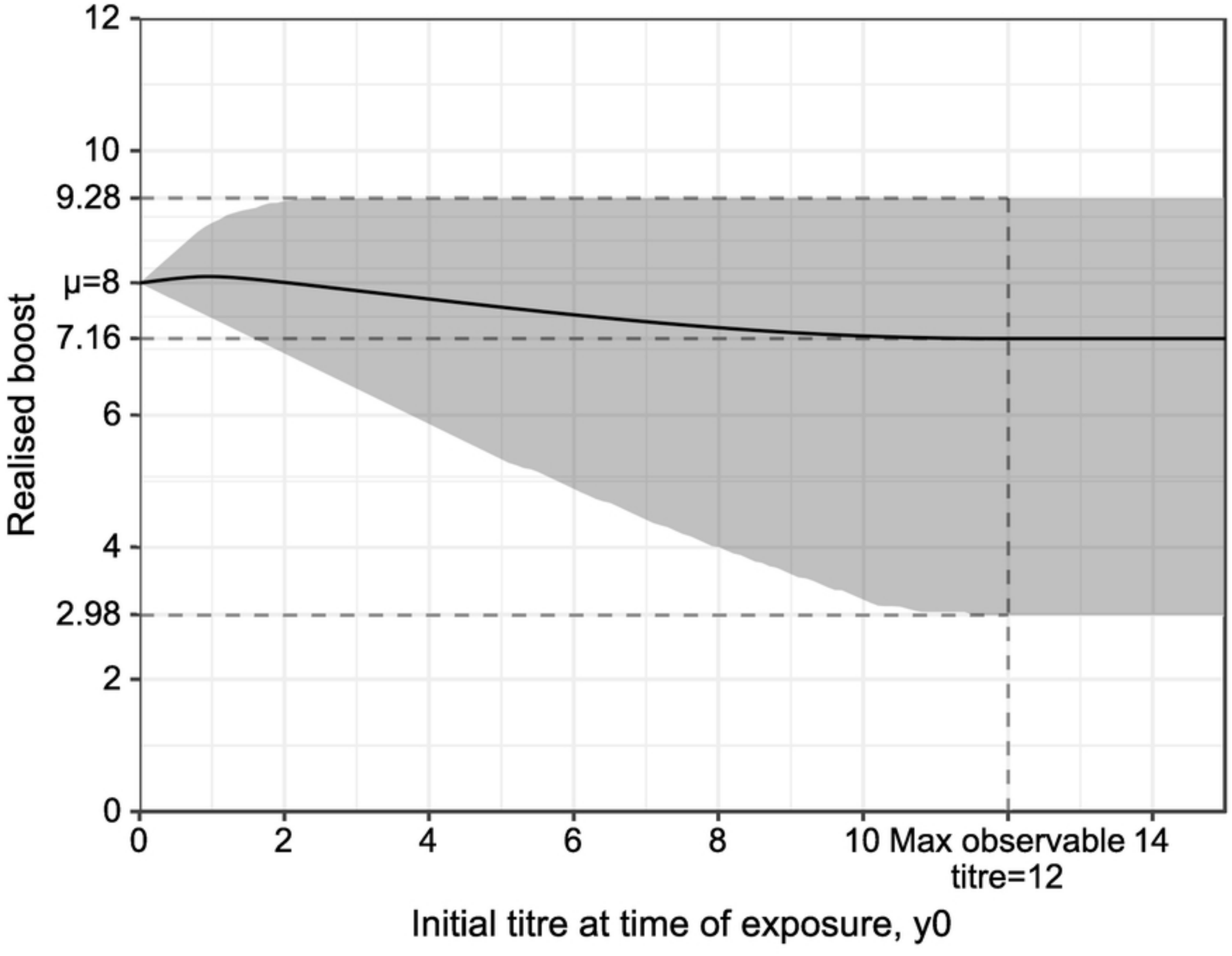
12
10
9.28
μ=8
7.16
6
4
2.98
2
0
Realised boost
0
2
4
6
8
10 Max observable titre=12
14
Initial titre at time of exposure, y0

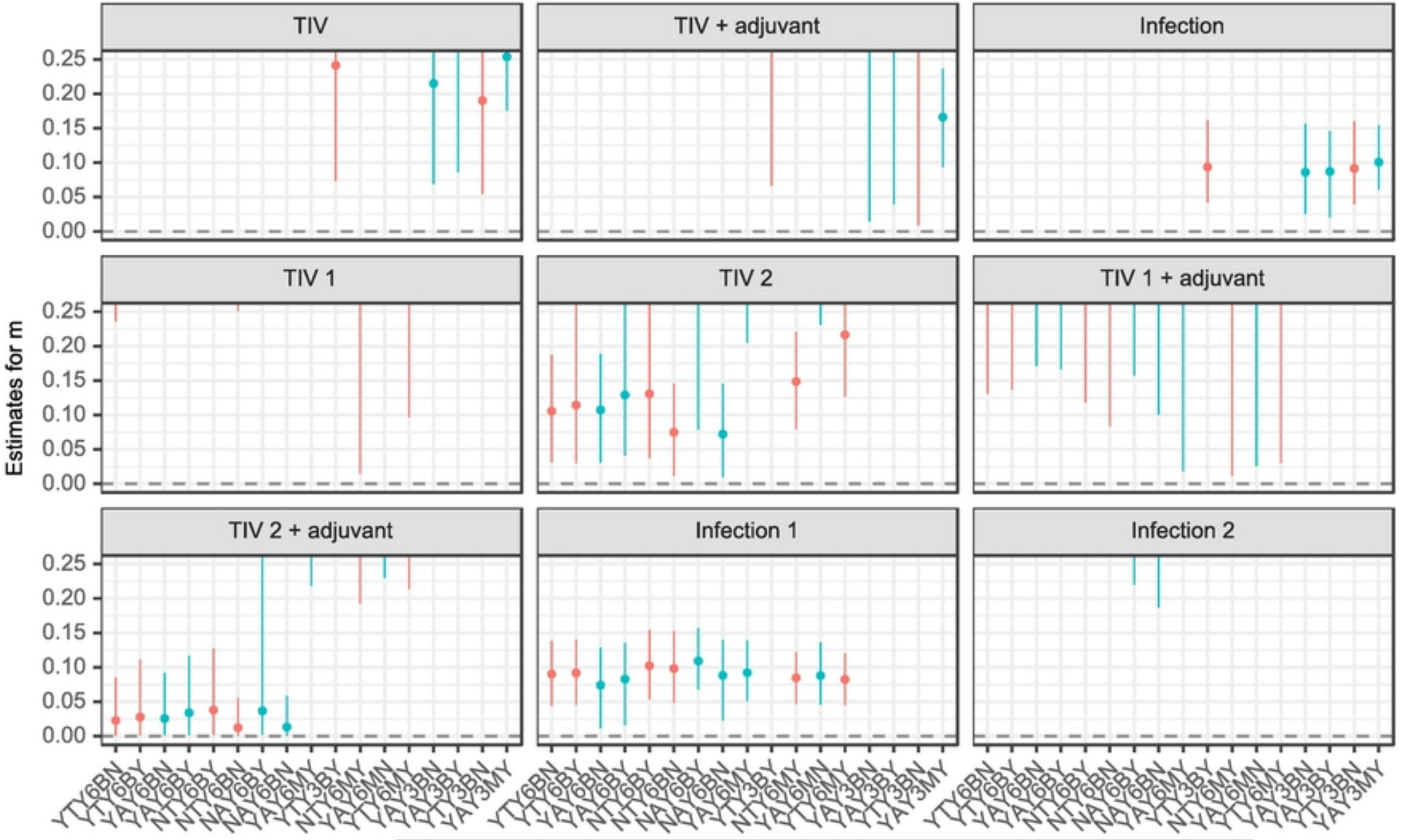

Cross Reactivity

- Universal
- Type specific

Mechanism	Antigenic seniority	Cross reactivity	Priming	Typed exposures	Waning	Titre dependent boosting
Option 1	Yes	Type specific	Yes	3types	Biphasic	Yes
Option 2	No	All	No	6types	Monophasic	No

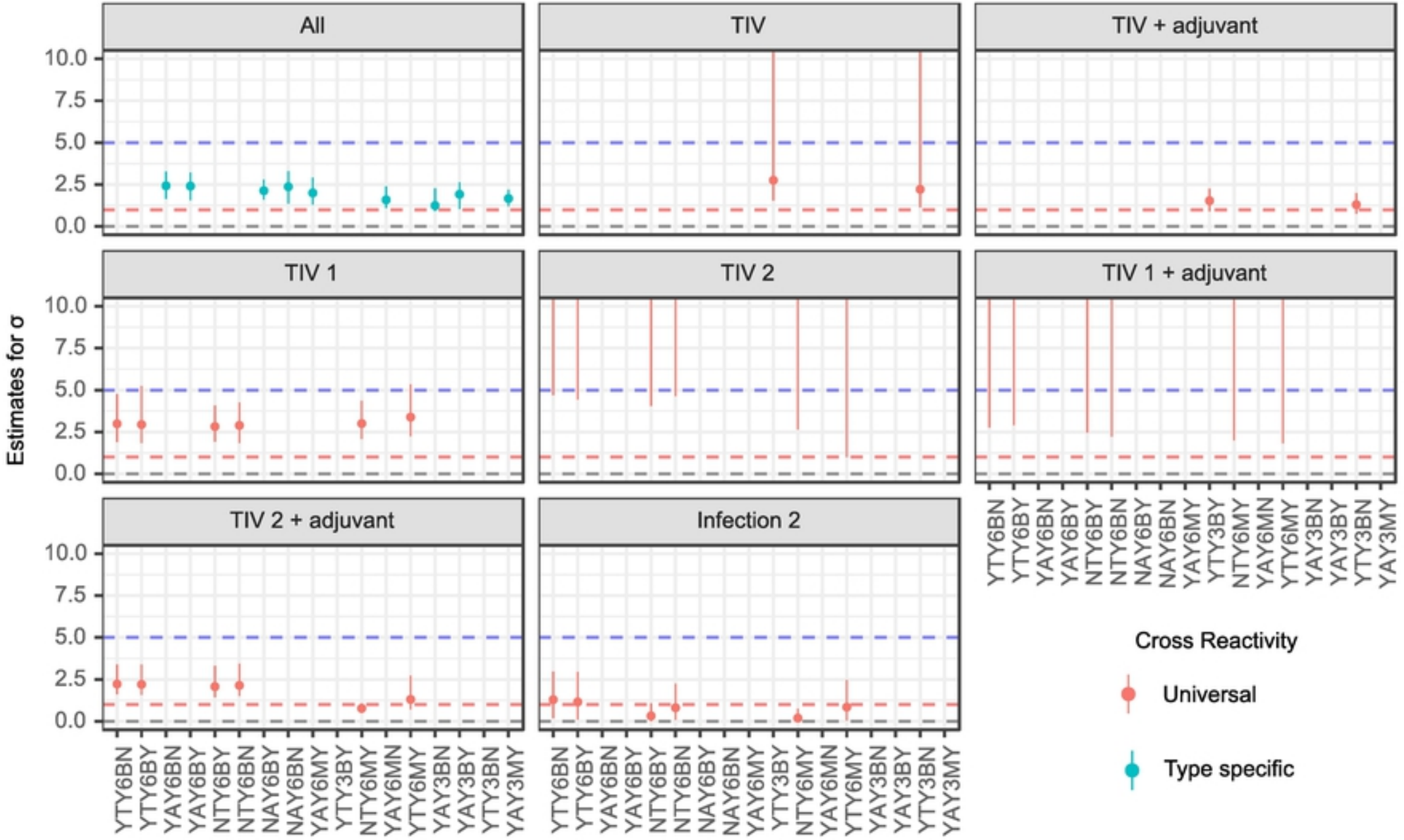

Mechanism	Antigenic seniority	Cross reactivity	Priming	Typed exposures	Waning	Titre dependent boosting
Option 1	Yes	Type specific	Yes	3types	Biphasic	Yes
Option 2	No	All	No	6types	Monophasic	No

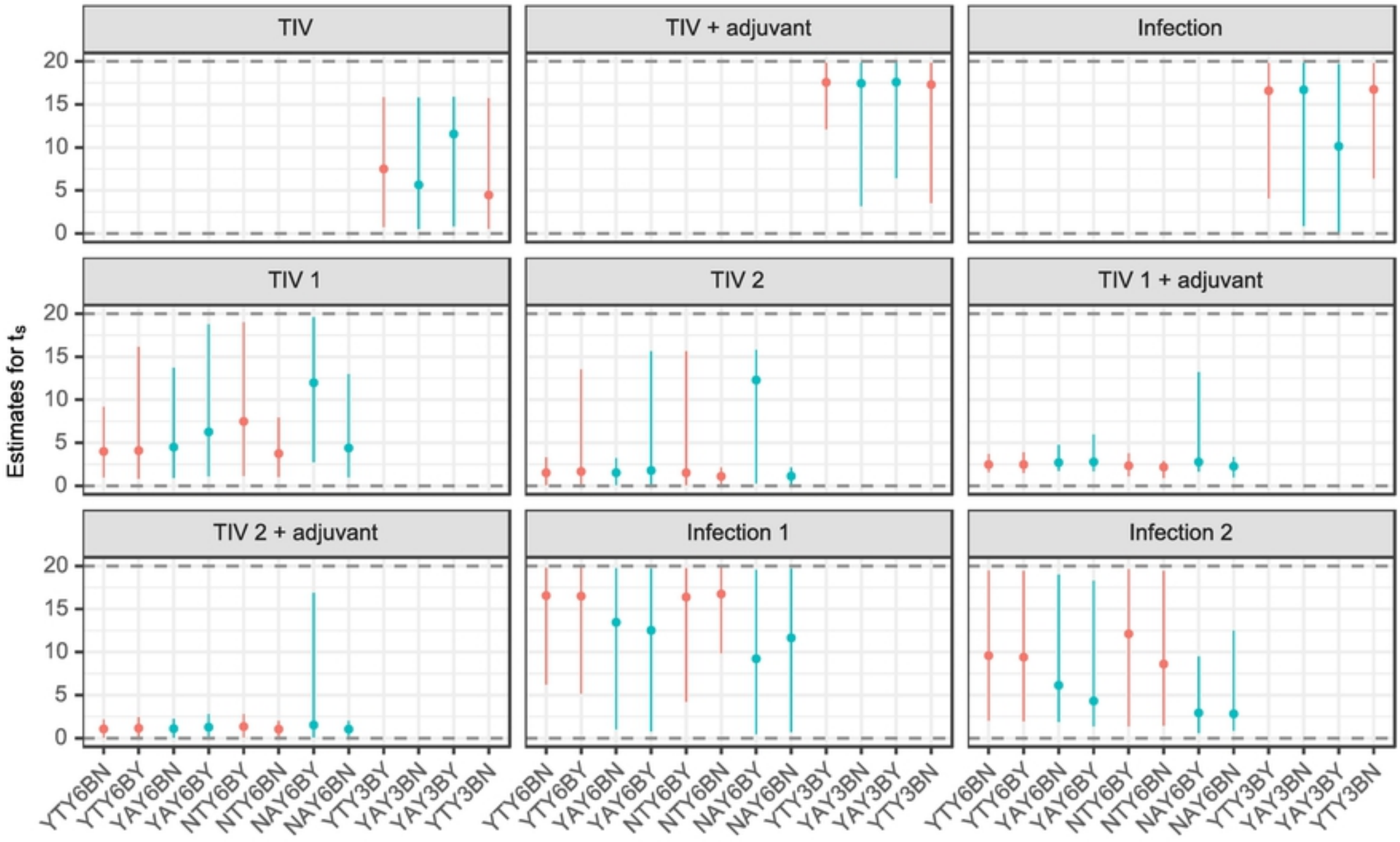

Mechanism	Antigenic seniority	Cross reactivity	Priming	Typed exposures	Waning	Titre dependent boosting
Option 1	Yes	Type specific	Yes	3types	Biphasic	Yes
Option 2	No	All	No	6types	Monophasic	No

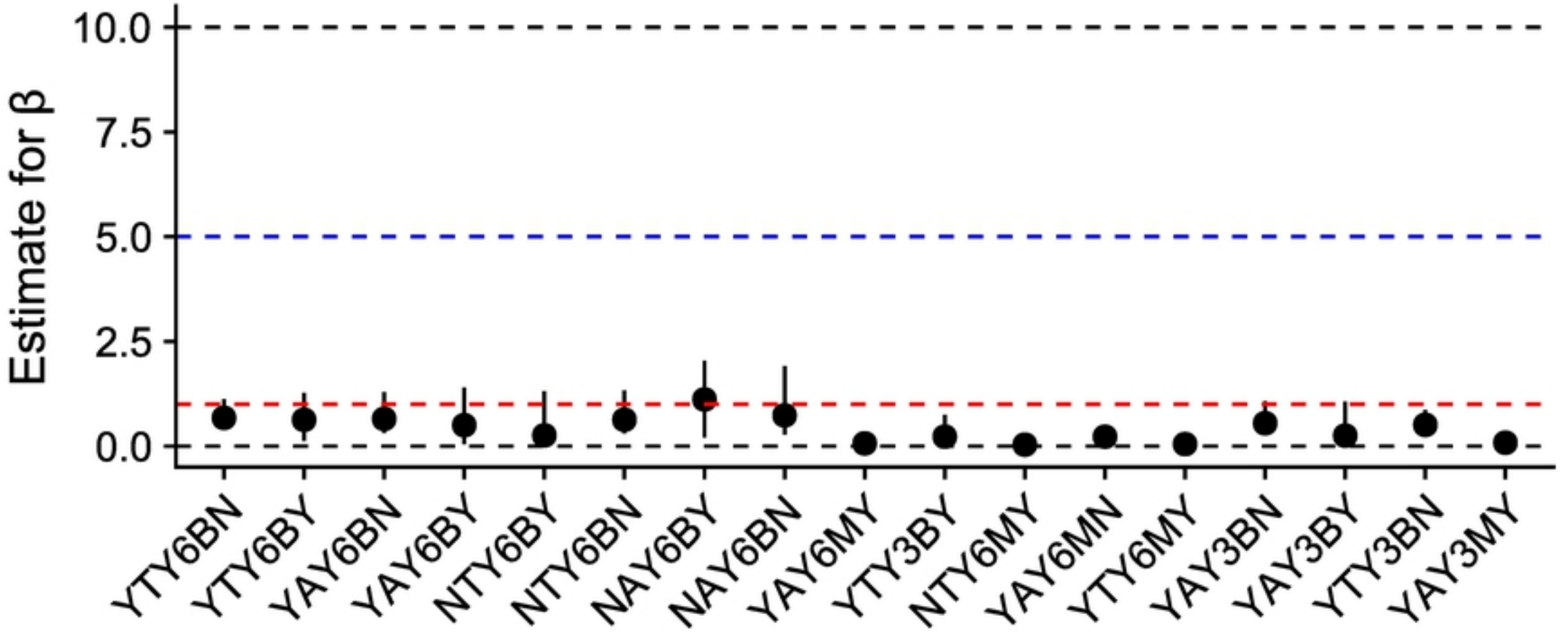

Mechanism	Antigenic seniority	Cross reactivity	Priming	Typed exposures	Waning	Titre dependent boosting
Option 1	Yes	Type specific	Yes	3types	Biphasic	Yes
Option 2	No	All	No	6types	Monophasic	No

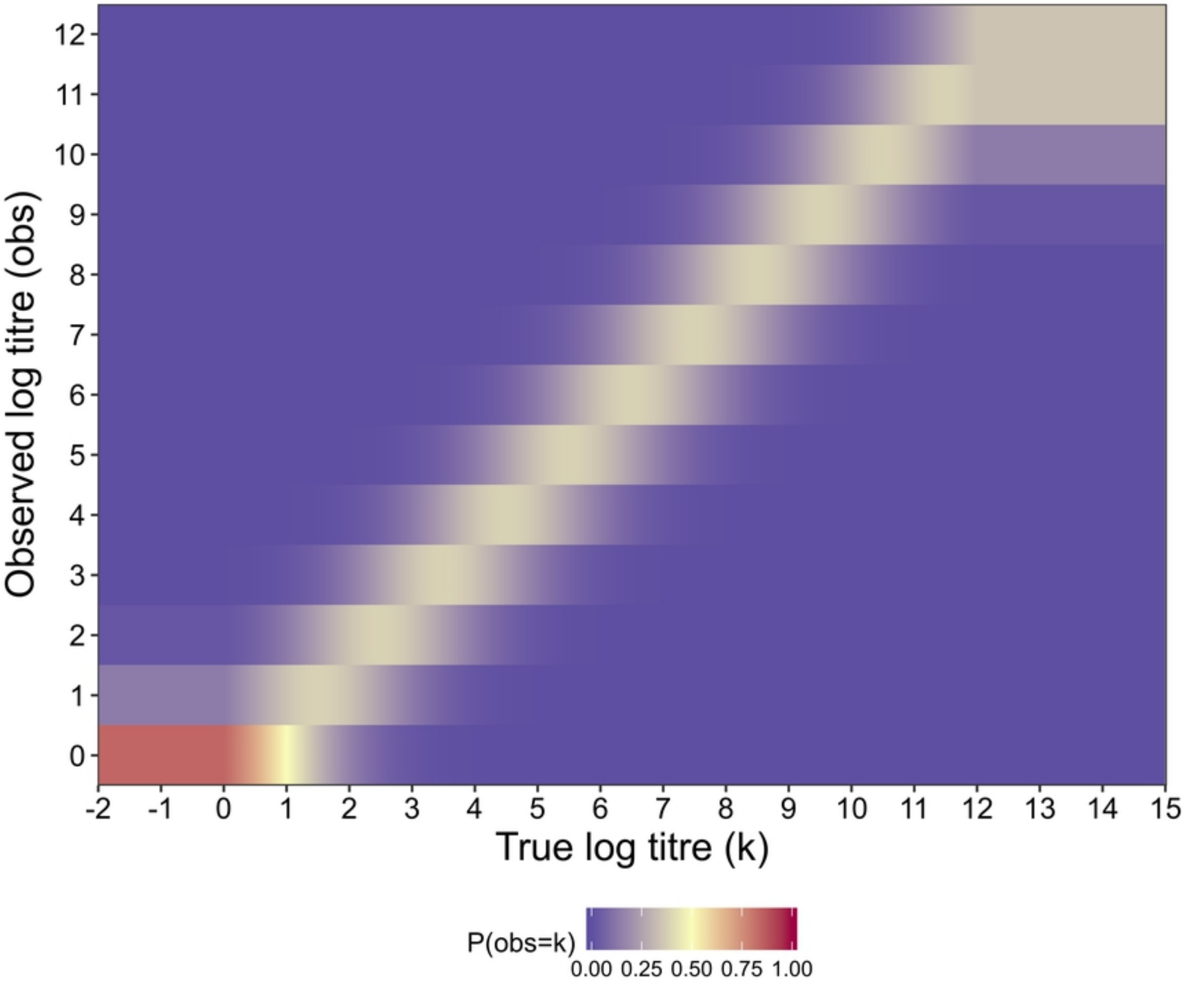
Observed log titre (obs)
12
11
10
9
8
7
6
5
4
3
2
1
0
-2
-1
0
1
2
3
4
5
6
7
8
9
10
11
12
13
14
15
True log titre (k)
P(obs=k)
0.00 0.25 0.50 0.75 1.00